國 立 交 通 大 學

電信工程研究所

碩 士 論 文

利用漸近解分析內嵌週期性金屬圓柱介質波導
之色散特性

Dispersion Analysis of Sidewall Dielectric Loading with

Embedded Lattice of Pins using Asymptotic Solution

研究生：邱怡嘉　　　　　　(Yi-Jia Chiou)

指導教授：黃謀勤 博士 (Dr. Malcolm Ng Mou Kehn)

中 華 民 國　　102 年　　9 月　　4 日

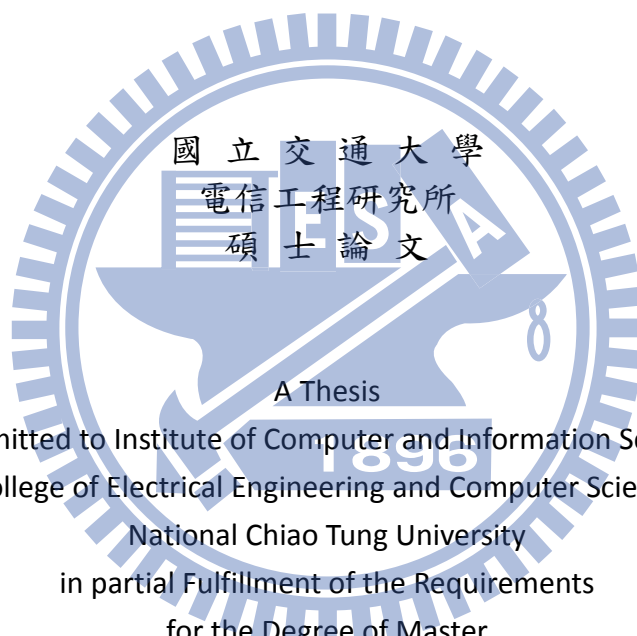利用漸近解分析內嵌週期性金屬圓柱介質波導之色散特性

Dispersion Analysis of Sidewall Dielectric Loading with Embedded Lattice of Pins using Asymptotic Solution

研 究 生：邱怡嘉 　　　　Student：Yi - Jia Chiou

指導教授：黃謀勤 　　　　Advisor：Malcolm Ng Mou Kehn

國 立 交 通 大 學

電信工程研究所

碩 士 論 文

A Thesis

Submitted to Institute of Computer and Information Science

College of Electrical Engineering and Computer Science

National Chiao Tung University

in partial Fulfillment of the Requirements

for the Degree of Master

in

Communication Engineering

September 2013

Hsinchu, Taiwan, Republic of China

中華民國一〇二年九月

利用漸近解分析內嵌週期性金屬圓柱介質波導之色散特性

學生:邱怡嘉　　　　　　　　　　　　　　　　指導教授:黃謀勤 博士

國立交通大學電信工程研究所碩士班

摘　　要

　　近來，有非常多的研究著重於電磁能隙結構(Electromagnetic Bandgap, EBG)，其特性最廣為人知便是在頻率截止帶相當於一高阻抗表面，有著抑制表面波的效果。除此之外，電磁能隙結構有些甚至放置在平行板波導的空隙中去實現高頻率波導特性。[1] 類似的概念也可以從矩形波導中發現。而還有一種新的複合材料，人們稱之為"針床"也已經被廣泛研究。其特性就類似於上述我們所說的 EBG 結構。不僅如此，我們可以發現此種結構應用在中脊波導，其原因在於此結構可近似模擬出高阻抗邊界條件；當我們放置一脊面於平行板波導中間、並讓周圍環繞著無限多(假想)的週期性金屬圓柱，當空氣隙小於四分之一波長時，那些規律無限多金屬圓柱形成了相當於理想磁導體(PMC)的平面，使得 TEM 波只會隨著中脊(ridge)而傳。

　　而這些年來，也有許多的研究是將一些填充物放置在空波導中，藉此量測波導的傳播特性、並且填充方式從最簡單的放置介質到插入一些介質層去做阻抗匹配並探討其特性。在此篇論文中，我們主要採用將空波導兩旁的介質放置入規律的

金屬長柱（理想導體），並且利用漸近解的方式去分析其特徵方程式；分析出特徵方程式之後再用模擬軟體去跑出其色散圖。由 HFSS 及 CST 吻合的色散圖來推斷其模擬結果是正確的，搭配 MATLAB 結果，來分析其特性。

在分析此結構之前，我們會先介紹另一較單純結構：在介質基座裡，想像其中嵌有無限週期性排列金屬柱、利用電磁場的概念下去分析推導，並用漸近解取得其特徵方程式；接著用模擬軟體 CST、HFSS 跑出其色散圖，並將其結果與橫向共振技術(Transverse Resonance Technique, TRT)得到的特性方程式用 MATLAB 模擬出的色散圖做比較，藉此來證明其漸近解的可靠性與準確性，同時解釋選擇此種場論分析的目的。

Dispersion Analysis of Sidewall Dielectric Loading with Embedded Lattice of Pins

using asymptotic solution

Student : Yi Jia Chiou   Advisor : Dr. Malcolm Ng Mou Kehn

Institute of Communications Engineering

National Chiao Tung University

ABSTRACT

There are so many researches focusing on Electromagnetic band-bap structure (EBG) recently; for their well-known characteristic of being as a high-impedance surface in frequency stop-band that can suppress surface waves. Besides, EBG structure can be used to realize a new high-frequency waveguide in the gap between the parallel plate waveguides. The similar concept can also be found in the rectangular waveguide. [1]

Recently, a new type of novel meta-surfaces, which is called "pin-lattice" or "bed-of-nails" is being widely researched.[2] Its characteristics are similar to those of EBG structures. [3][4]

Furthermore, we can see that the "bed-of-nails" structure is also applied in ridge gap waveguide. The reason of this structure being used is because that can usually mimic the ideal impedance boundary. When we put a ridge in the parallel plate and surrounded infinitely periodic pins, the "bed-of-nails" structure would be similar with PMC (Perfectly Magnetic Conducting) surface when the air gap is smaller than quarter-wavelength and let TEM wave propagate following on the ridge.[5]

In recent years, the insertion of additional structures into empty waveguide has

been practiced a lot, which can discuss about the characteristics of the propagation through the measurement of the waveguides. Furthermore, the insertion has ranging from the simplest use of dielectric fillings for reduction of cutoff frequency to the plugging in of dielectric layers to serve as impedance match-tunners. In this paper, we use the structure that is a waveguide filling the dielectric in the sidewall and loading with uniform embedded lattice of metallic pins (Perfect Electric Conductor, PEC). Next, we analyzed its characteristic equation by asymptotic solution, and simulated with the tools to get the dispersion diagrams. By agreements of simulating results in CST and HFSS, we can assume its accuracy, and we will analyze the characteristics with the MATLAB tool.

On the other hand, we will introduce another simpler structure before the sidewall loaded with embedded pins waveguide; first, we imagine that there is a dielectric grounded plane filling with infinitely periodic array of metallic pins. Next, we derive it by the concept of electromagnetics and get the characteristic equation through the asymptotic solution. Then, we compare the result through the simulated tools with the result of the Transverse Resonance Technique (TRT), and we can get the agreement of the results and the dependability of the asymptotic solution.[2] Meanwhile, we will explain the objective of choosing this field analyzing method.

好意見、也能告訴我們準確的方向幫助我們解除迷惘。謝謝瑜秀，從大學時期就跟我很有緣份，也在找工作時期給予非常多寶貴建議、替我打氣，讓我倍感溫馨。謝謝奕心與學群常來我們實驗室聊天，也會給我們很多協助與建議。要謝謝的十分的多；除了謝謝實驗室老師學長同學們，我也想特別謝謝劉明彰老師、李長綱老師、喻超凡老師。以及許恆通老師。

最重要的，我必須得感謝父母給我的支持與鼓勵、無私奉獻，並將我帶到這世界上讓我體會這一切。在我準備論文階段，總是給我打氣讓我感到無後顧之憂的準備著學業。還有我阿姨總是提供我們美食與溫暖的另一個窩，為我們補身體的同時，也讓我們心裡很溫暖。
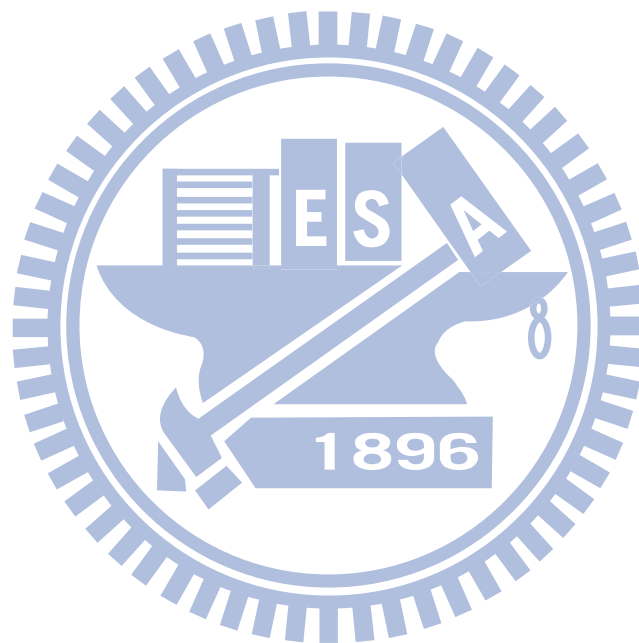
謝謝哥哥姐姐常跟我說空話讓我人生道路不空虛，在關鍵時刻也能給予有建設性的意見，陪我大吃大喝、陪我開心陪我難過，帶我去馬殺雞放鬆身心靈。謝謝衣婷與東元也常打氣鼓勵我，讓我更有信心。

謝謝每一個給予我幫助的人，為我打氣的人，因為你們的溫暖字句，我才能一直保有動力與方向。

最後，我想謝謝我家的狗狗傑利，我覺得很歉疚沒能在離開時陪在身邊，甚至口試完才能知道已經離開的事實，你是我們家的夥伴，也是我最常在家裡陪伴著你，好想和你分享這一切的喜悅，只希望你可以了無遺憾在另一個地方繼續看著我努力，謝謝你的可愛，還有九年
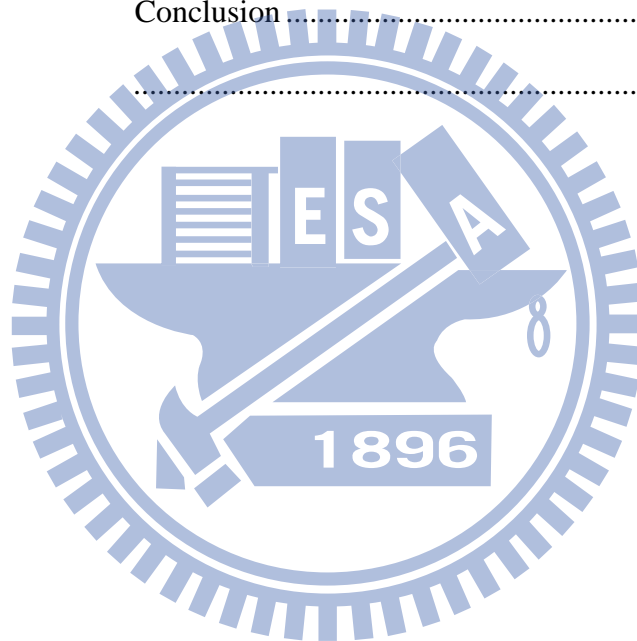
多的陪伴，我想你是我們家的、我的精神依靠與寄託。希望你已經沒有了病痛，在康復的九個多月裡，我相信你是很開心的。你會一直存在我們家的每個人心裡。

TABLE OF CONTENTS

LIST OF FIGURES

I. Introduction

Usually, the hollow waveguide can be manufactured in two parts that are joined together, but there would be a big problem which is that we cannot ensure good electrical contact in the joints. When it comes to radio frequency transmission, the micro-strip lines are commonly used as well, but the losses increase with frequency, as well as the power handling capability being reduced.

Therefore, there is a need for new waveguides or transmission lines operating at high frequencies, in particular above 30 GHz. There exist already some waveguides particularly intended for use at high frequencies. Such a waveguide is the so-called substrate integrated waveguide (SIW), as described in [6].

However, these waveguides still suffer from losses due to the substrate, and the metallized via holes represent a complication that is expensive to manufacture.

The first conceptual attempt to realize magnetic conductivity (in the form of high surface impedance) was the so-called soft and hard surfaces. For its abnormal characteristic which is the equivalent of magnetic conductivity, such materials are often referred to as meta-materials.

Recently, there has been a new type of novel meta-surfaces, which is called "pin-lattice" or "bed-of-nails".[2] Its characteristics are similar to those of EBG (electromagnetic band-gap) structures, which are well-known for suppressing surface wave propagation in a specific band. [3][4]

The "bed-of-nails" structure can also be applied in the ridge gap waveguide.[7] The reason of this structure being used is because it can usually mimic the ideal impedance boundary. When we put a ridge in the parallel plate and surround it with an infinite array of periodic pins, and when the air gap is smaller than

quarter-wavelength, TEM waves propagate along the ridge.[1]

II. Theory

2-1 Modal Analysis of a Periodic Pins Array within a Grounded Dielectric Substrate

In this section, we analyze a basic structure being simply a grounded dielectric substrate and seek to demonstrate that by the concept of assuming TEM solution in the dielectric region perpendicular to the slab surface, the presence of the pin lattice within the dielectric slab can be effectively taken into account in an asymptotic manner. As in, the solution approaches exactness as the period of the lattice tends to zero. Besides, we demonstrated the characteristic equation with a key concept which is we assume the TEM solution within the dielectric region to the normal direction of the slab surface. That is to say, it will only be sense by the vertical y-oriented embedded pins in the substrate when TM^y modes. Which means the TE^y modes won't feel them. Hence, we derive the equation only for TM^y modes.

In the next section, we use the classical analysis by vector potentials and we assume a "TEM-to-slab-surface-normal" solution inside the pin-lattice layer. In that way, the approach is reasonable only when the pin-period is diminishingly small, i.e. the density of the pins would be likely to infinity. As mentioned, we use the key concept, and let k_d, the wavenumber in the dielectric, to equal k_{yd}, the wavenumber along the y-direction in the dielectric, perpendicular to the surface. The reason for this is because the wave within the space between adjacent pins was forced to propagate

along them, and acting as a transmission line, thereby tantamount to being TEM to the direction perpendicular to the slab surface.

Figure 1 below shows the structure of the lattice of grounded metallic pins embedded within a slab of dielectric host.
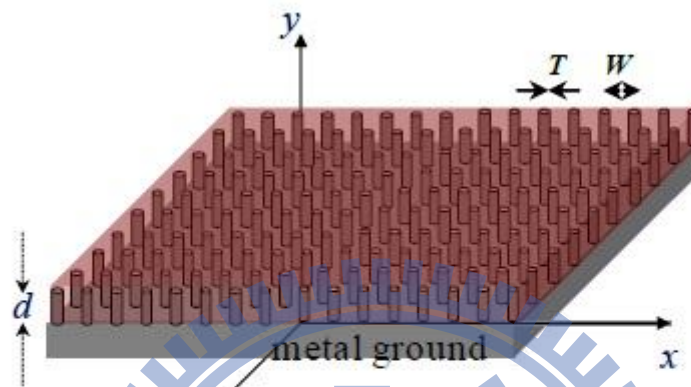
Fig.1   Lattice of grounded metallic pins, or bed-of-nails, embedded within a slab of dielectric host

2-2 Transverse Resonance Technique and Characteristic Equation Demonstrated by Vector-potential Method

This section presents the derivation of the TM mode characteristic equation in the substrate without any pins embedded by using the vector-potential method. Next step, we then let $k_d = k_{yd}$. This turns out to be exactly the same as using the transverse resonance technique (TRT).[5] Before commencing with the vector-potential method, we first introduce the TRT. Fig. 2 below shows the transverse equivalent network of the TE_{0N} waveguide.

In the transverse resonance method the cross section of a traveling wave structure is represented as a transmission line network. The method can be illustrated with Fig.2, which shows a simple example with a conventional TE$_{0N}$ waveguide.

For this structure, a TE wave travels in the x direction with propagation constant γ_x, and the Z$_{0N}$ represents the characteristic impedance of the transmission line. At any point, when we look into the impedance line of the transverse network from the positive x direction would be equal and it would be opposite when we look into the negative x direction. This is the same applied to admittance. Which follows the continuity that the components of **E** and **H** are tangential to a plane orthogonal to the transverse transmission line, also means that x = constant plane in Fig.2.

Another way to state the impedance relationship is that the sum of the two impedances that are observed by opposite directions from a point on the line must be canceled to zero.

From the above discussion it is clear that one needs to know both the impedance of the equivalent line and the aperture impedance in order to apply transverse resonance.

Transverse resonance technique is a method to find the propagation constant of many practical traveling wave structures.
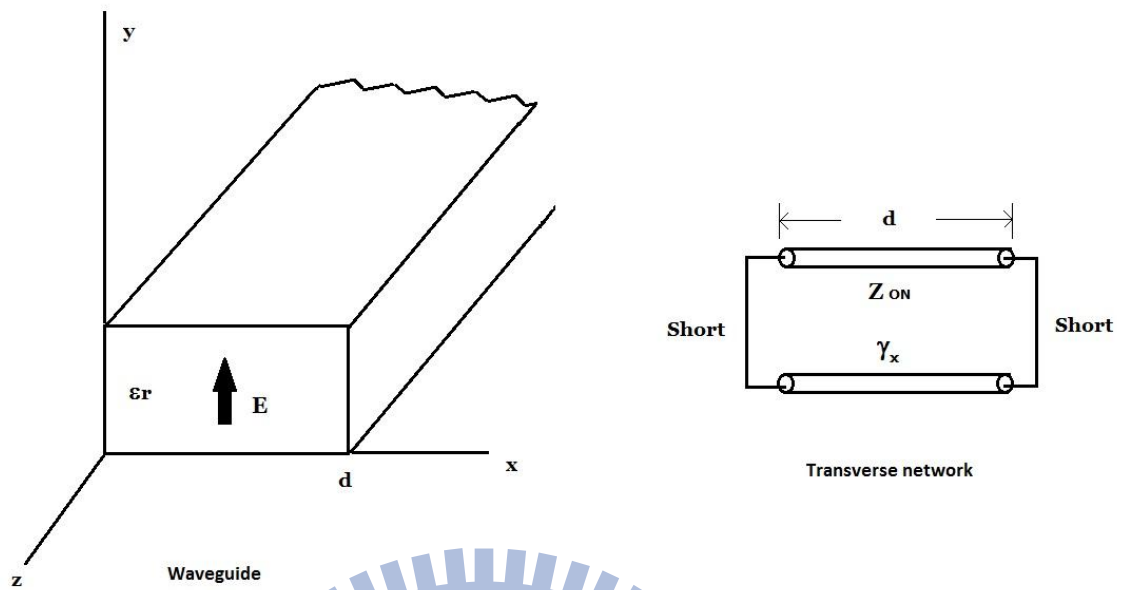
Fig.2   Transverse equivalent network of TE_{0N} waveguide

After briefly introducing the TRT, the vector-potential method is discussed. Fig.3 below shows the grounded dielectric substrate with thickness d and (μ_d, ε_d) material. It is along the x-z plane, and y-axis is the normal direction.
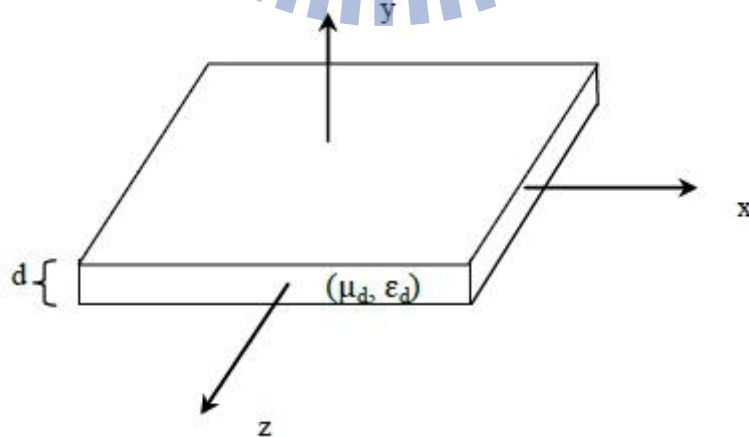
Fig.3   Grounded dielectric substrate with thickness d and (μ_d, ε_d) material

The various field components of the TM^y modes are stated as follow. [7]

$$E_x = \frac{1}{j\omega\mu\varepsilon}\frac{\partial^2 A_y}{\partial x \partial y}\ ;\ E_y = \frac{1}{j\omega\mu\varepsilon}\left(\frac{\partial^2}{\partial y} + k^2\right)A_y\ ;\ E_z = \frac{1}{j\omega\mu\varepsilon}\frac{\partial^2 A_y}{\partial y \partial z} \tag{a1}$$

$$H_x = -\frac{1}{\mu}\frac{\partial A_y}{\partial z}\ ;\ \ H_y = 0\ ;\ \ H_z = \frac{1}{\mu}\frac{\partial A_y}{\partial x} \tag{a2}$$

For the slab region: script "d": $0 < y < d$

$$A_y^d(x, 0 < y < d, z) = \left[C_x^d e^{-jk_{xd}x}\ |_{x<0} + D_x^d e^{+jk_{xd}x}\ |_{x<0}\right]\times$$

$$\times\left[C_y^d \cos(k_{yd}y) + D_y^d \sin(k_{yd}y)\right]\left[C_z^d e^{-jk_{zd}z}\ |_{z>0} + D_z^d e^{+jk_{zd}z}\ |_{z<0}\right] \tag{Eq-1}$$

For the upper (air) region: script "0": $y > d$

$$A_y^0(x, y > d, z) = \left[C_x^0 e^{-jk_{x0}x}\ |_{x>0} + D_x^0 e^{+jk_{x0}x}\ |_{x<0}\right]\times$$

$$\times e^{-jk_{y0}(y-d)}\times\left[C_z^0 e^{-jk_{z0}z}\ |_{z>0} + D_x^0 e^{+jk_{z0}z}\ |_{z<0}\right] \tag{Eq-2}$$

The boundary conditions are stated as follow.

$$E_x^d(x, y = 0, z) = 0 \tag{BC-1a}$$

$$E_z^d(x, y = 0, z) = 0 \tag{BC-1b}$$

$$E_x^d(x, y = d, z) = E_x^0(x, y = d, z) \tag{BC-2a}$$

$$E_z^d(x, y = d, z) = E_z^0(x, y = d, z) \tag{BC-2b}$$

$$H_x^d(x, y = d, z) = H_x^0(x, y = d, z) \tag{BC-3a}$$

$$H_z^d(x, y = d, z) = H_z^0(x, y = d, z) \quad\quad\quad\quad\quad\text{(BC-3b)}$$

By (a1), (a2), (Eq-1), and (Eq-2), we can state these equations of each region as below:

$$E_x^d = \frac{1}{j\omega\mu_d\varepsilon_d}\frac{\partial^2 A_y^d}{\partial x\partial y} = \frac{jk_{xd}k_{yd}}{j\omega\mu_d\varepsilon_d}\Big[D_x^d e^{+jk_{xd}x}\mid_{x<0} -C_x^d e^{-jk_{xd}x}\mid_{x>0}\Big]\times$$

$$\times\Bigg[D_y^d \cos(k_{yd}y) - C_y^d \sin(k_{yd}y)\Bigg]\Big[C_z^d e^{-jk_{zd}z} + D_z^d e^{+jk_{zd}z}\Big] \quad\quad\text{(Eq-3)}$$

Then applying (BC-1a): we get $D_y^d = 0$.

Next,

$$E_z^d = \frac{1}{j\omega\mu_d\varepsilon_d}\frac{\partial^2 A_y^d}{\partial y\partial z} = \frac{jk_{zd}k_{yd}}{j\omega\mu_d\varepsilon_d}\Big[C_x^d e^{-jk_{xd}x}\mid_{x>0} +D_x^d e^{+jk_{xd}x}\mid_{x<0}\Big]\times$$

$$\times\Bigg[D_y^d \cos(k_{yd}y) - C_y^d \sin(k_{yd}y)\Bigg]\Big[D_z^d e^{+jk_{zd}z} - C_z^d e^{-jk_{zd}z}\Big] \quad\quad\text{(Eq-4)}$$

Next,

$$E_x^0 = \frac{1}{j\omega\mu_0\varepsilon_0}\frac{\partial^2 A_y^0}{\partial x\partial y} = \frac{jk_{x0}(-jk_{y0})}{j\omega\mu_0\varepsilon_0}\Big[D_x^0 e^{+jk_{x0}x}\mid_{x<0} -C_x^0 e^{-jk_{x0}x}\mid_{x>0}\Big]\times$$

$$\times e^{-jk_{y0}(y-d)}\times\Big[C_z^0 e^{-jk_{z0}z} + D_z^0 e^{+jk_{z0}z}\Big] \quad\quad\quad\quad\quad\text{(Eq-5)}$$

Then, applying (BC-2a):

$$\frac{k_{zd}k_{yd}}{\omega\mu_d\varepsilon_d}\Big[D_x^d e^{+jk_{xd}x}\mid_{x<0} -C_x^d e^{-jk_{xd}x}\mid_{x>0}\Big]\Big[-C_y^d \sin(k_{yd}d)\Big]\Big[C_z^d e^{-jk_{zd}z} + D_z^d e^{+jk_{zd}z}\Big] =$$

$$= \frac{k_{x0}(k_{y0})}{j\omega\mu_0\varepsilon_0}\Big[D_x^0 e^{+jk_{x0}x}\mid_{x<0} -C_x^0 e^{-jk_{x0}x}\mid_{x>0}\Big]\Big[C_z^0 e^{-jk_{z0}z} + D_z^0 e^{+jk_{z0}z}\Big] \quad\text{(Eq-6)}$$

Next,

$$E_z^0 = \frac{1}{j\omega\mu_d\varepsilon_d}\frac{\partial^2 A_y^0}{\partial y\partial z} = \frac{-jk_{y0}jk_{z0}}{j\omega\mu_0\varepsilon_0}\Big[C_x^0 e^{-jk_{x0}x}\mid_{x>0} +D_x^0 e^{+jk_{x0}x}\mid_{x<0}\Big]\times$$

$$\times e^{-jk_{y0}(y-d)} \times \left[D_z^0 e^{+jk_{z0}z} - C_z^0 e^{-jk_{z0}z} \right] \qquad \text{(Eq-7)}$$

Then, applying (BC-2b):

$$\frac{k_{zd}k_{yd}}{\omega\mu_d\varepsilon_d} \left[C_x^d e^{-jk_{xd}x} \big|_{x>0} + D_x^d e^{+jk_{xd}x} \big|_{x<0} \right] \left[-C_y^d \sin(k_{yd}d) \right] \left[D_z^d e^{+jk_{zd}z} - C_z^d e^{-jk_{zd}z} \right] =$$

$$= \frac{k_{y0}k_{z0}}{j\omega\mu_0\varepsilon_0} \left[C_x^0 e^{-jk_{x0}x} \big|_{x>0} + D_x^0 e^{+jk_{x0}x} \big|_{x<0} \right] \left[D_z^0 e^{+jk_{z0}z} - C_z^0 e^{-jk_{z0}z} \right] \qquad \text{(Eq-8)}$$

Next, need H_x and H_z in both layers:

$$H_x^d = -\frac{1}{\mu_d}\frac{\partial A_y^d}{\partial z} = \frac{jk_{zd}}{\mu_d} \left[C_x^d e^{-jk_{xd}x} \big|_{x>0} + D_x^d e^{+jk_{xd}x} \big|_{x<0} \right] \left[C_y^d \cos(k_{yd}y) \right] \left[C_z^d e^{-jk_{zd}z} - D_z^d e^{+jk_{zd}d} \right]$$

$$\text{(Eq-9)}$$

$$H_x^0 = -\frac{1}{\mu_0}\frac{\partial A_y^0}{\partial z} = \frac{jk_{z0}}{\mu_0} \left[C_x^0 e^{-jk_{x0}x} \big|_{x>0} + D_x^0 e^{+jk_{x0}x} \big|_{x<0} \right] \times e^{-jk_{y0}(y-d)} \times \left[C_z^0 e^{-jk_{z0}z} + D_z^0 e^{+jk_{z0}z} \right]$$

$$\text{(Eq-10)}$$

$$H_z^0 = \frac{1}{\mu_0}\frac{\partial A_y^0}{\partial x} = \frac{jk_{x0}}{\mu_0} \left[D_x^0 e^{+jk_{x0}x} \big|_{x<0} - C_x^0 e^{-jk_{x0}x} \big|_{x>0} \right] \times e^{-jk_{y0}(y-d)} \times \left[C_z^0 e^{-jk_{z0}z} + D_z^0 e^{+jk_{z0}z} \right]$$

$$\text{(Eq-11)}$$

Then applying (BC-3a):

$$\frac{k_{zd}}{\mu_d} \left[C_x^d e^{-jk_{xd}x} \big|_{x>0} + D_x^d e^{+jk_{xd}x} \big|_{x<0} \right] \left[C_y^d \cos(k_{yd}d) \right] \left[C_z^d e^{-jk_{zd}z} - D_z^d e^{+jk_{zd}z} \right] =$$

$$= \frac{k_{z0}}{\mu_0} \left[C_x^0 e^{-jk_{x0}x} \big|_{x>0} + D_x^0 e^{+jk_{x0}x} \big|_{x<0} \right] \left[C_z^0 e^{-jk_{z0}z} - D_z^0 e^{+jk_{z0}z} \right] \qquad \text{(Eq-12)}$$

And applying (BC-3b):

$$\frac{k_{xd}}{\mu_d} \left[D_x^d e^{+jk_{xd}x} \big|_{x<0} - C_x^d e^{-jk_{xd}x} \big|_{x>0} \right] \left[C_y^d \cos(k_{yd}d) \right] \left[C_z^d e^{-jk_{zd}z} + D_z^d e^{+jk_{zd}z} \right] =$$

$$= \frac{k_{x0}}{\mu_0} \left[D_x^0 e^{+jk_{x0}x} \big|_{x<0} - C_x^0 e^{-jk_{x0}x} \big|_{x>0} \right] \left[C_z^0 e^{-jk_{z0}z} + D_z^0 e^{+jk_{z0}z} \right] \qquad \text{(Eq-13)}$$

Dividing (Eq-6) by (Eq-13):

$$-\frac{k_{yd}}{\omega\varepsilon_d}\Big[\tan(k_{yd}d)\Big] = \frac{k_{y0}}{j\omega\varepsilon_0} \qquad\qquad\text{(Eq-14)}$$

Then we set $k_{y0} = -j\alpha_{y0}$,

Here, we only consider the slow wave, so we think about the **"–ja"** situation only,

and then we will get:

$$\frac{k_{yd}}{\omega\varepsilon_d}\Big[\tan(k_{yd}d)\Big] = \frac{\alpha_{y0}}{\omega\varepsilon_0} \qquad\qquad\text{(Eq-15)}$$

Next, we let $k_{yd} = k_d = \omega\sqrt{\mu_d\varepsilon_d}$ [9], and the above equation becomes:

$$\frac{k_d}{\omega\varepsilon_d}\Big[\tan(k_d d)\Big] = \frac{\alpha_{y0}}{\omega\varepsilon_0} \Rightarrow$$

$$\Rightarrow \alpha_{y0} = \frac{\varepsilon_0}{\varepsilon_d}k_d\tan(k_d d) = \frac{k_0\sqrt{\mu_d\varepsilon_d}}{\varepsilon_d}\tan(k_d d) = \frac{k_0\sqrt{\mu_d}}{\sqrt{\varepsilon_d}}\tan(k_d d) \qquad\text{(Eq-16)}$$

By dividing (Eq-8) by (Eq-12) above, we can obtain the exact same equation.

However, we still need one more correction factor for the real case which the metallic-pins aren't being infinite.

It is fairly presumed that the electric fields on the substrate surface may be corrected by an incremental factor $w/(w + t)$, where w is the distance between two pins, and t is the diameter of the pin, yielding

$$\alpha_{y0} = \frac{w}{w+t}\frac{k_0\sqrt{\mu_d}}{\sqrt{\varepsilon_d}}\tan(k_d d) \qquad\qquad\text{(Eq-17)}$$

2-3 Simulation result

We get the characteristic equation above, and then use the simulate tools CST and Matlab to observe their agreement. Fig.4 below shows the simulation result. The blue

square would be the Matlab result, and the purple star represents the CST result. We can find out that they have excellent agreement in every mode.
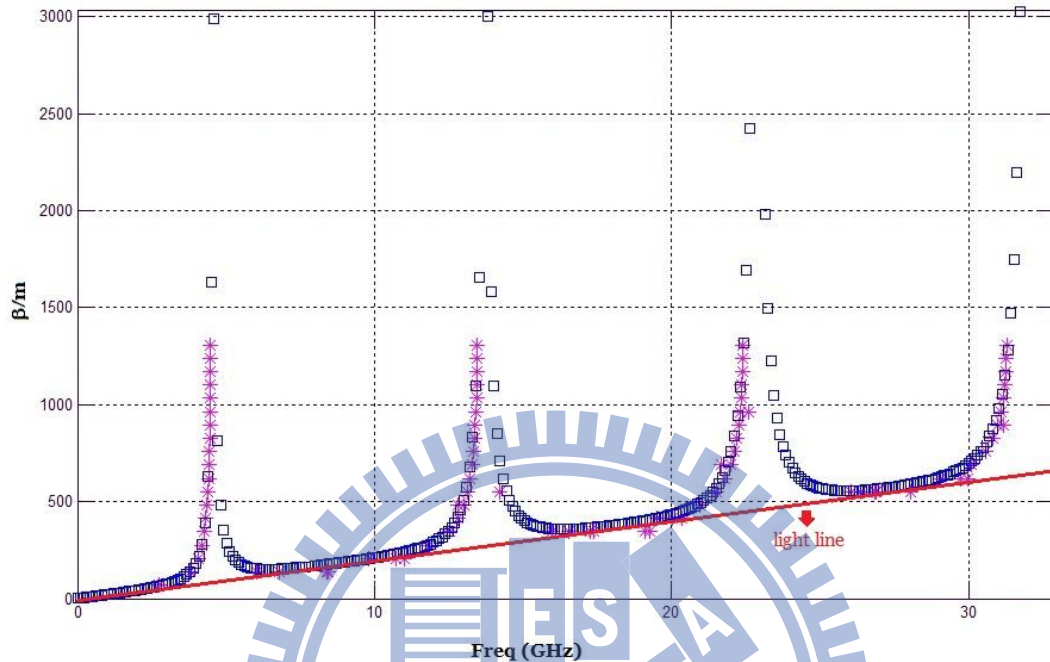
Fig.4   Comparison of Matlab and CST simulation results

By this result, we can prove that our vector-potential method matches to the TRT (Transverse Resonance Technique) solution.

2-4 Rigorous analysis of partially dielectric-loaded rectangular waveguide using vector potential method

Here, we will demonstrate treatment methods of inhomogeneously dielectric-loaded rectangular waveguide.

2-4-1 Analytical Modal Field Solutions

First, the inhomogeneously dielectric-loaded rectangular waveguide consists of an

empty rectangular waveguide with two E-plane sidewalls (when fundamental modal electric field is parallel to these side walls) which are coated with a dielectric lining of a certain thickness $d = \dfrac{\lambda_{TEM}}{4\sqrt{\varepsilon_r - 1}}$, where $\lambda_{TEM} = \dfrac{c}{f_{TEM}}$, with f_{TEM} being the designated TEM frequency.

The geometry of the structure is shown in the figure below.
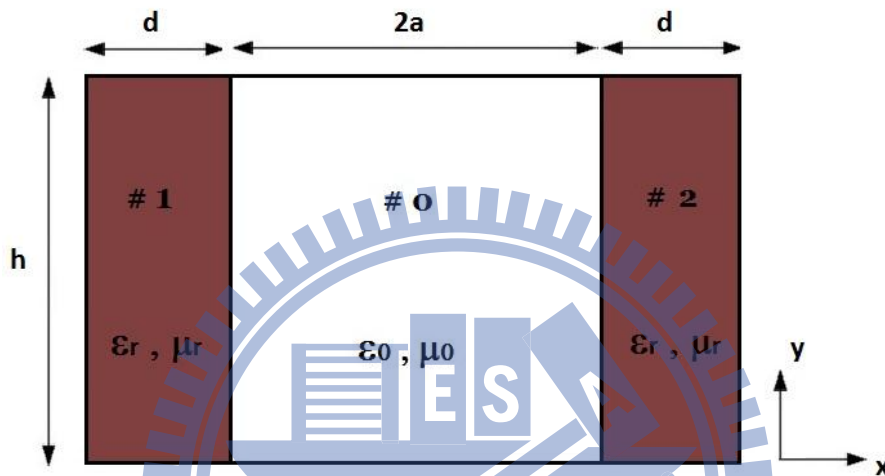
Fig.5   Geometry of partially dielectric-loaded rectangular waveguide

Fig.6 (a) and (b) below shows the cross-sectional view of rectangular waveguide with dielectric sidewall loading embedded with a lattice of pins.

Fig.7 below represents the perspective view of pin-lattice sidewall-loaded waveguide.
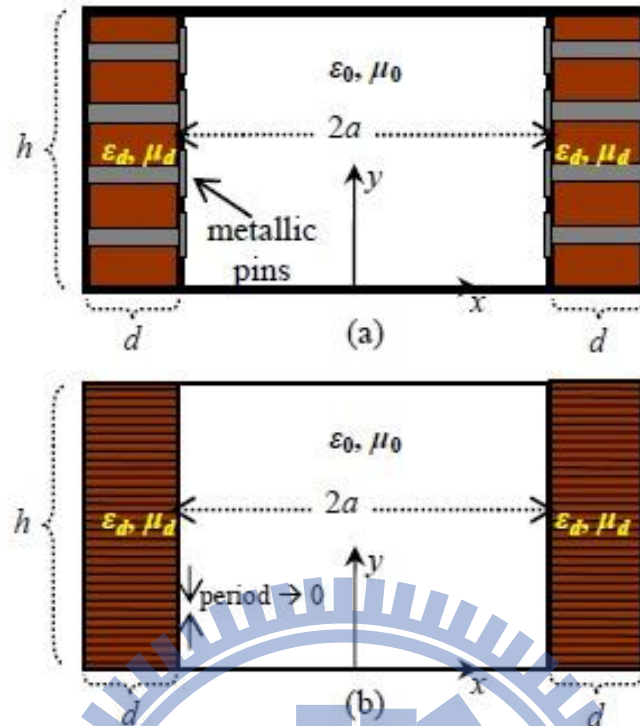
Fig.6　Cross-sectional view of a rectangular waveguide with dielectric sidewall loading embedded with a lattice of pins (a.k.a. bed-of-nails), (a). finite periodicity, and (b). infinitesimal period for asymptotic treatment.
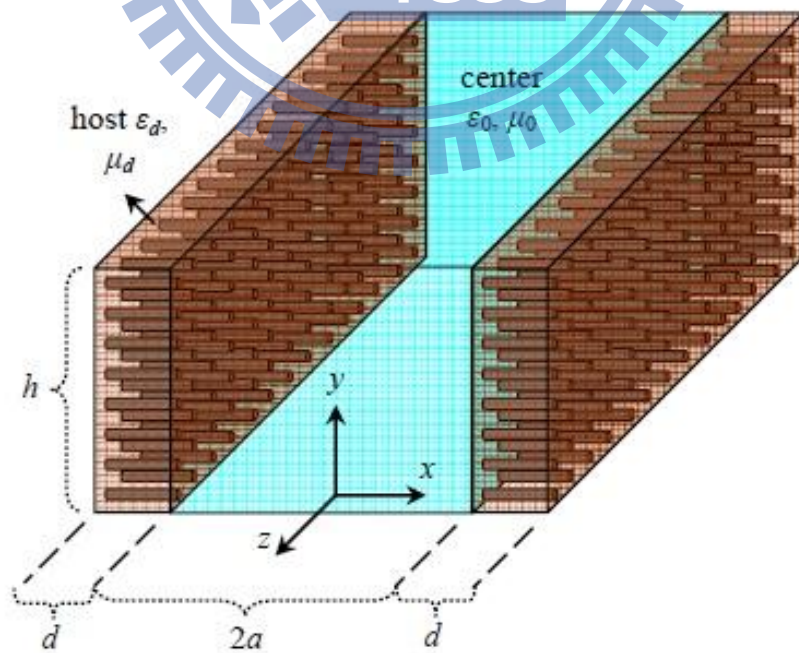
Fig.7　Perspective view of pin-lattices sidewall-loaded waveguide

The modal fields within this inhomogeneously-filled waveguide are neither TE^z nor TM^z, but rather are mode configurations that are combinations of these two modes. Such combined modes are referred to as hybrid modes or longitudinal section electric (*LSE*) or longitudinal section magnetic (*LSM*) modes.

2-4-2 Case (I): LSE^x or TE^x mode (for above geometry, with x normal to discontinuity interface)

(A) For central freespace region: $-a \le x \le a$: subscript '0'

$$F_x^0(-a \le x \le a, y, z) = \left[C_x^0 \cos\left(k_{x0} x\right) + D_x^0 \sin\left(k_{x0} x\right) \right]\left[C_y^0 \cos\left(k_{y0} y\right) + D_y^0 \sin\left(k_{y0} y\right) \right] A_z^0 e^{-\gamma_z z}$$

(IA1)

with

$$\gamma_z = \alpha_z + j k_z$$

(IA2a) which is valid throughout

and

$$k_{x0}^2 + k_{y0}^2 - \gamma_z^2 = \omega^2 \mu_0 \varepsilon_0 = k_0^2$$

(IA2bi) for generally lossy case

$$k_{x0}^2 + k_{y0}^2 + k_z^2 = \omega^2 \mu_0 \varepsilon_0 = k_0^2$$

(IA2bii) for lossless case with $\alpha_z = 0$

(B) For dielectric region: $-(a+d) \le x \le a$ and $a < x < a+d$

(1) Left dielectric region: $-(a+d) \le x \le a$ (superscript or subscript '1')

$$F_x^{d1}[-(a+d) \le x \le -a, y, z] = \left\{ C_x^{d1} \cos\left[k_{xd}^{(1)}(x+a+d) \right] + D_x^{d1} \sin\left[k_{xd}^{(1)}(x+a+d) \right] \right\}$$

$$\times \left\{ C_y^{d1} \cos\left[k_{yd}^{(1)} y \right] + D_y^{d1} \sin\left[k_{yd}^{(1)} y \right] \right\} A_z^{d1} e^{-\gamma_z z}$$

(IB1a)

with

$$\left[k_{xd}^{(1)} \right]^2 + \left[k_{yd}^{(1)} \right]^2 - \gamma_z^2 = \omega^2 \mu_d \varepsilon_d = k_d^2 \qquad \text{(IB1bi) for generally lossy case}$$

$$\left[k_{xd}^{(1)} \right]^2 + \left[k_{yd}^{(1)} \right]^2 + k_z^2 = \omega^2 \mu_d \varepsilon_d = k_d^2 \qquad \text{(IB1bii) for lossless case with } \alpha_z = 0$$

(2)Right dielectric region: $a \le x \le a+d$ (superscript or subscript '2')

$$F_x^{d2}[a \le x \le a+d, y, z] = \left\{ C_x^{d2} \cos\left[k_{xd}^{(2)}(x-a-d) \right] + D_x^{d2} \sin\left[k_{xd}^{(2)}(x-a-d) \right] \right\}$$

$$\times \left\{ C_y^{d2} \cos\left[k_{yd}^{(2)} y \right] + D_y^{d2} \sin\left[k_{yd}^{(2)} y \right] \right\} A_z^{d2} e^{-\gamma_z z} \qquad \text{(IB2a)}$$

with

$$\left[k_{xd}^{(2)} \right]^2 + \left[k_{yd}^{(2)} \right]^2 - \gamma_z^2 = \omega^2 \mu_d \varepsilon_d = k_d^2 \qquad \text{(IB2bi) for generally lossy case}$$

and

$$\left[k_{xd}^{(2)} \right]^2 + \left[k_{yd}^{(2)} \right]^2 + k_z^2 = \omega^2 \mu_d \varepsilon_d = k_d^2 \qquad \text{(IB2bii) for lossless case with } \alpha_z = 0$$

(C)Boundary Conditions:

(1) $E_z^{d1}\left[x = -(a+d), 0 \le y \le h, z \right] = E_z^{d2}\left[x = a+d, 0 \le y \le h, z \right] = 0 \qquad \text{(IC1)}$

(2a) $E_z^{d1}\left[x = -(a+d) \le x \le -a, y = 0, z \right] = E_z^{d1}\left[x = -(a+d) \le x \le -a, y = h, z \right] = 0$

$$\text{(IC2a)}$$

(2b) $E_z^{d2}\left[a \le x \le a+d, y = 0, z \right] = E_z^{d2}\left[a \le x \le a+d, y = h, z \right] = 0 \qquad \text{(IC2b)}$

(3) $E_z^0\left(-a \le x \le a, y = 0, z \right) = E_z^0\left(-a \le x \le a, y = h, z \right) = 0 \qquad \text{(IC3)}$

(4a) $E_z^{d1}\left(x = -a, 0 \le y \le h, z \right) = E_z^0\left(x = -a, 0 \le y \le h, z \right) \qquad \text{(IC4a)}$

(4b) $E_z^{d2}\left(x = a, 0 \le y \le h, z \right) = E_z^0\left(x = a, 0 \le y \le h, z \right) \qquad \text{(IC4b)}$

(5a) $H_z^{d1}\left(x = -a, 0 \le y \le h, z \right) = H_z^0\left(x = -a, 0 \le y \le h, z \right) \qquad \text{(IC5a)}$

(5b) $H_z^{d2}\left(x=a,0\le y\le h,z\right)=H_z^0\left(x=a,0\le y\le h,z\right)$ (IC5b)

(6) $E_y^{d1}\left[x=-(a+d),0\le y\le h,z\right]=E_y^{d2}\left(x=a+d,0\le y\le h,z\right)=0$ (IC6)

(7a) $E_x^{d1}\left[-(a+d)\le x\le-a,y=0,z\right]=E_x^{d1}\left[-(a+d)\le x\le-a,y=h,z\right]=0$ (IC7a)

(7b) $E_x^{d2}\left[a\le x\le a+d,y=0,z\right]=E_x^{d2}\left(a\le x\le a+d,y=h,z\right)=0$ (IC7b)

(8) $E_x^0\left(-a\le x\le a,y=0,z\right)=E_x^0\left(-a\le x\le a,y=h,z\right)=0$ (IC8)

(9a) $E_y^{d1}\left(x=-a,0\le y\le h,z\right)=E_y^0\left(x=-a,0\le y\le h,z\right)$ (IC9a)

(9b) $E_y^{d2}\left(x=a,0\le y\le h,z\right)=E_y^0\left(x=a,0\le y\le h,z\right)$ (IC9b)

(10a) $H_y^{d1}\left(x=-a,0\le y\le h,z\right)=H_y^0\left(x=-a,0\le y\le h,z\right)$ (IC10a)

(10b) $H_y^{d2}\left(x=a,0\le y\le h,z\right)=H_y^0\left(x=a,0\le y\le h,z\right)$ (IC10b)

For LSE^x mode, we know that

$$E_z=\frac{1}{\varepsilon}\frac{\partial F_x}{\partial y}$$

Therefore, we have:

Using (IA1):

$$E_z^0=\frac{1}{\varepsilon_0}\frac{\partial F_x^0}{\partial y}=\frac{k_{y0}}{\varepsilon_0}\left[C_x^0\cos(k_{x0}x)+D_x^0\sin(k_{x0}x)\right]\left[D_y^0\cos(k_{y0}y)-C_y^0\sin(k_{y0}y)\right]A_z^0e^{-\gamma_z z}$$

Apply (IC3):

$$E_z^0\left(-a\le x\le a,y=0,z\right)=0\Rightarrow D_y^0=0$$

$$E_z^0\left(-a\le x\le a,y=h,z\right)=0\Rightarrow k_{y0}=\frac{n\pi}{h}$$

Thus $E_z^0=\frac{k_{y0}}{\varepsilon_0}\left[C_x^0\cos(k_{x0}x)+D_x^0\sin(k_{x0}x)\right]\left[-C_y^0\sin(k_{y0}y)\right]A_z^0e^{-\gamma_z z}$ (I1)

Using (IB1):

$$E_z^{d1} = \frac{1}{\varepsilon_d} \frac{\partial F_x^{d1}}{\partial y} =$$

$$= \frac{k_{yd}^{(1)}}{\varepsilon_d} \left\{ C_x^{d1} \cos\left[k_{xd}^{(1)}(x+a+d) \right] + D_x^{d1} \sin\left[k_{xd}^{(1)}(x+a+d) \right] \right\} \times$$

$$\times \left\{ D_y^{d1} \cos\left[k_{yd}^{(1)} y \right] - C_y^{d1} \sin\left[k_{yd}^{(1)} y \right] \right\} A_z^{d1} e^{-\gamma_z z}$$

Apply (IC1): $E_z^{d1}\left[x = -(a+d) \right] = 0 \Rightarrow C_x^{d1} = 0$

Apply (IC2a): $\begin{cases} E_z^{d1}(y=0) = 0 \Rightarrow D_y^{d1} = 0 \\ E_z^{d1}(y=h) = 0 \Rightarrow k_{yd}^{(1)} = \dfrac{n\pi}{h} \end{cases}$

Thus $E_z^{d1} = \dfrac{k_{yd}^{(1)}}{\varepsilon_d} \left\{ D_x^{d1} \sin\left[k_{xd}^{(1)}(x+a+d) \right] \right\} \left\{ -C_y^{d1} \sin\left[k_{yd}^{(1)} y \right] \right\} A_z^{d1} e^{-\gamma_z z}$ \hfill (I2)

Using (IB2):

$$E_z^{d2} = \frac{1}{\varepsilon_d} \frac{\partial F_x^{d2}}{\partial y} =$$

$$= \frac{k_{yd}^{(2)}}{\varepsilon_d} \left\{ C_x^{d2} \cos\left[k_{xd}^{(2)}(x-a-d) \right] + D_x^{d2} \sin\left[k_{xd}^{(2)}(x-a-d) \right] \right\} \times$$

$$\times \left\{ D_y^{d2} \cos\left[k_{yd}^{(2)} y \right] - C_y^{d2} \sin\left[k_{yd}^{(2)} y \right] \right\} A_z^{d2} e^{-\gamma_z z}$$

Apply (IC1): $E_z^{d2}\left[x = a+d \right] = 0 \Rightarrow C_x^{d2} = 0$

Apply (IC2b): $\begin{cases} E_z^{d2}(y=0) = 0 \Rightarrow D_y^{d2} = 0 \\ E_z^{d2}(y=h) = 0 \Rightarrow k_{yd}^{(2)} = \dfrac{n\pi}{h} \end{cases}$

Thus $E_z^{d2} = \dfrac{k_{yd}^{(2)}}{\varepsilon_d} \left\{ D_x^{d2} \sin\left[k_{xd}^{(2)}(x-a-d) \right] \right\} \left\{ -C_y^{d2} \sin\left[k_{yd}^{(2)} y \right] \right\} A_z^{d2} e^{-\gamma_z z}$ \hfill (I3)

Use (I1) and (I2) in (IC4a):

$$\frac{k_{y0}}{\varepsilon_0}\Big[C_x^0\cos(k_{x0}a)-D_x^0\sin(k_{x0}a)\Big]\Big[-C_y^0\sin(k_{y0}y)\Big]A_z^0e^{-\gamma_z z}=$$

$$=\frac{k_{yd}^{(1)}}{\varepsilon_d}\Big\{D_x^{d1}\sin\Big[k_{xd}^{(1)}d\Big]\Big\}\Big\{-C_y^{d1}\sin\Big[k_{yd}^{(1)}y\Big]\Big\}A_z^{d1}e^{-\gamma_z z}$$

Since $k_{y0}=k_{yd}^{(1)}=n\pi\big/h$, thus

$$\frac{C_y^0 A_z^0}{\varepsilon_0}\Big[C_x^0\cos(k_{x0}a)-D_x^0\sin(k_{x0}a)\Big]=\frac{D_x^{d1}C_y^{d1}A_z^{d1}}{\varepsilon_d}\sin\Big[k_{xd}^{(1)}d\Big]\qquad(I4)$$

Use (I1) and (I3) in (IC4b):

$$\frac{k_{y0}}{\varepsilon_0}\Big[C_x^0\cos(k_{x0}a)+D_x^0\sin(k_{x0}a)\Big]\Big[-C_y^0\sin(k_{y0}y)\Big]A_z^0e^{-\gamma_z z}=$$

$$=\frac{k_{yd}^{(2)}}{\varepsilon_d}\Big\{D_x^{d2}\sin\Big[k_{xd}^{(2)}d\Big]\Big\}\Big\{C_y^{d2}\sin\Big[k_{xd}^{(2)}y\Big]\Big\}A_z^{d2}e^{-\gamma_z z}$$

Since $k_{y0}=k_{yd}^{(2)}=n\pi\big/h$, thus

$$-\frac{C_y^0 A_z^0}{\varepsilon_0}\Big[C_x^0\cos(k_{x0}a)+D_x^0\sin(k_{x0}a)\Big]=\frac{D_x^{d2}C_y^{d2}A_z^{d2}}{\varepsilon_d}\sin\Big[k_{xd}^{(2)}d\Big]\qquad(I5)$$

Also for LSE^X modes,

$$H_z=\frac{1}{j\omega\mu\varepsilon}\frac{\partial^2 F_x}{\partial x\partial z}$$

Hence using (IA1), whose $D_y^0=0$:

$$H_z^0=\frac{1}{j\omega\mu_0\varepsilon_0}\frac{\partial^2 F_x^0}{\partial x\partial z}=-\frac{k_{x0}\gamma_z}{j\omega\mu_0\varepsilon_0}\Big[D_x^0\cos(k_{x0}x)-C_x^0\sin(k_{x0}x)\Big]C_y^0\cos(k_{y0}y)A_z^0e^{-\gamma_z z}\quad(I6)$$

Using (IB1) with its $C_x^{d1}=D_y^{d1}=0$

$$H_z^{d1}=\frac{1}{j\omega\mu_d\varepsilon_d}\frac{\partial^2 F_x^{d1}}{\partial x\partial z}=-\frac{k_{xd}^{(1)}\gamma_z}{j\omega\mu_d\varepsilon_d}\Big\{D_x^{d1}\cos\Big[k_{xd}^{(1)}(x+a+d)\Big]\Big\}\Big\{C_y^{d1}\cos\Big[k_{yd}^{(1)}y\Big]\Big\}A_z^{d1}e^{-\gamma_z z}$$

$$(I7)$$

Using (IB2) with its $C_x^{d2}=D_y^{d2}=0$

$$H_z^{d2} = \frac{1}{j\omega\mu_d\varepsilon_d}\frac{\partial^2 F_x^{d2}}{\partial x\partial z} = -\frac{k_{xd}^{(2)}\gamma_z}{j\omega\mu_d\varepsilon_d}\left\{D_x^{d2}\cos\left[k_{xd}^{(2)}(x-a-d)\right]\right\}\left\{C_y^{d2}\cos\left[k_{yd}^{(2)}y\right]\right\}A_z^{d2}e^{-\gamma_z z}$$

$$(\text{I8})$$

Use (I6) and (I7) in (IC5a):

$$-\frac{k_{x0}\gamma_z}{j\omega\mu_0\varepsilon_0}\left[C_x^0\sin(k_{x0}a)+D_x^0\cos(k_{x0}a)\right]C_y^0\cos(k_{y0}y)A_z^0e^{-\gamma_z z} =$$

$$= -\frac{k_{xd}^{(1)}\gamma_z}{j\omega\mu_d\varepsilon_d}\left\{D_x^{d1}\cos\left[k_{xd}^{(1)}d\right]\right\}\left\{C_y^{d1}\cos\left[k_{yd}^{(1)}y\right]\right\}A_z^{d1}e^{-\gamma_z z}$$

Again with $k_{y0} = k_{yd}^{(1)} = n\pi/h$,

$$\frac{k_{x0}}{\mu_0\varepsilon_0}\left[C_x^0\sin(k_{x0}a)+D_x^0\cos(k_{x0}a)\right]C_y^0A_z^0 = \frac{k_{xd}^{(1)}D_x^{d1}C_y^{d1}A_z^{d1}}{\mu_d\varepsilon_d}\cos\left[k_{xd}^{(1)}d\right] \qquad (\text{I9})$$

Use (I6) and (I8) in (IC5b):

$$-\frac{k_{x0}\gamma_z}{j\omega\mu_0\varepsilon_0}\left[D_x^0\cos(k_{x0}a)-C_x^0\sin(k_{x0}a)\right]C_y^0\cos(k_{y0}y)A_z^0e^{-\gamma_z z} =$$

$$= -\frac{k_{xd}^{(2)}\gamma_z}{j\omega\mu_d\varepsilon_d}\left\{D_x^{d2}\cos\left[k_{xd}^{(2)}d\right]\right\}\left\{C_y^{d2}\cos\left[k_{yd}^{(2)}y\right]\right\}A_z^{d2}e^{-\gamma_z z}$$

Again with $k_{y0} = k_{yd}^{(2)} = n\pi/h$,

$$\frac{k_{x0}}{\mu_0\varepsilon_0}\left[D_x^0\cos(k_{x0}a)-C_x^0\sin(k_{x0}a)\right]C_y^0A_z^0 = \frac{k_{xd}^{(2)}D_x^{d2}C_y^{d2}A_z^{d2}}{\mu_d\varepsilon_d}\cos\left[k_{xd}^{(2)}d\right] \qquad (\text{I10})$$

Divide (I4) by (I9), we have

$$\frac{\mu_0\left[C_x^0\cos(k_{x0}a)-D_x^0\sin(k_{x0}a)\right]}{k_{x0}\left[C_x^0\sin(k_{x0}a)+D_x^0\cos(k_{x0}a)\right]} = \frac{\mu_d\tan\left[k_{xd}^{(1)}d\right]}{k_{xd}^{(1)}} \qquad (\text{I11})$$

Divide (I5) by (I10), we have

$$\frac{\mu_0\left[C_x^0\cos(k_{x0}a)+D_x^0\sin(k_{x0}a)\right]}{k_{x0}\left[C_x^0\sin(k_{x0}a)-D_x^0\cos(k_{x0}a)\right]} = \frac{\mu_d\tan\left[k_{xd}^{(2)}d\right]}{k_{xd}^{(2)}} \qquad (\text{I12})$$

Also for LSE^x mode,

$$E_y = -\frac{1}{\varepsilon}\frac{\partial F_x}{\partial z} \quad \text{and} \quad H_y = \frac{1}{j\omega\mu\varepsilon}\frac{\partial^2 F_x}{\partial x \partial y}$$

Thus, using (IB1) with its $C_x^{d1} = D_y^{d1} = 0$, we have

$$E_y^{d1} = -\frac{1}{\varepsilon_d}\frac{\partial F_x^{d1}}{\partial z} = \frac{\gamma_z}{\varepsilon_d}\left\{D_x^{d1}\sin\left[k_{xd}^{(1)}(x+a+d)\right]\right\}\times$$

$$\times\left\{C_y^{d1}\cos\left[k_{yd}^{(1)}\right]\right\}A_z^{d1}e^{-\gamma_z z} \tag{I13}$$

$$H_y^{d1} = \frac{1}{j\omega\mu_d\varepsilon_d}\frac{\partial^2 F_x^{d1}}{\partial x \partial y} =$$

$$= -\frac{k_{xd}^{(1)}k_{yd}^{(1)}}{j\omega\mu_d\varepsilon_d}\left\{D_x^{d1}\cos\left[k_{xd}^{(1)}(x+a+d)\right]\right\}\left\{C_y^{d1}\sin\left[k_{yd}^{(1)}y\right]\right\}A_z^{d1}e^{-\gamma_z z} \tag{I14}$$

Apply (IB2) with its $C_x^{d2} = D_y^{d2} = 0$,

$$E_y^{d2} = -\frac{1}{\varepsilon_d}\frac{\partial F_x^{d2}}{\partial z} = \frac{\gamma_z}{\varepsilon_d}\left\{D_x^{d2}\sin\left[k_{xd}^{(2)}(x-a-d)\right]\right\}\times$$

$$\times\left\{C_y^{d2}\cos\left[k_{yd}^{(2)}\right]\right\}A_z^d e^{2-\gamma_z z} \tag{I15}$$

$$H_y^{d2} = \frac{1}{j\omega\mu_d\varepsilon_d}\frac{\partial^2 F_x^{d2}}{\partial x \partial y} =$$

$$= -\frac{k_{xd}^{(2)}k_{yd}^{(2)}}{j\omega\mu_d\varepsilon_d}\left\{D_x^{d2}\cos\left[k_{xd}^{(2)}(x-a-d)\right]\right\}\left\{C_y^{d2}\sin\left[k_{yd}^{(2)}y\right]\right\}A_z^d e^{2-\gamma_z z} \tag{I16}$$

Apply (IA1) whose $D_y^0 = 0$,

$$E_y^0 = -\frac{1}{\varepsilon_0}\frac{\partial F_x^0}{\partial z} = \frac{\gamma_z}{\varepsilon_0}\left[C_x^0\cos(k_{x0}x)+D_x^0\sin(k_{x0}x)\right]C_y^0\cos(k_{y0}y)A_z^0 e^{-\gamma_z z} \tag{I17}$$

$$H_y^0 = \frac{1}{j\omega\mu_0\varepsilon_0}\frac{\partial F_x^0}{\partial x \partial y} =$$

$$= -\frac{k_{x0}k_{y0}}{j\omega\mu_0\varepsilon_0}\left[D_x^0\cos(k_{x0}x)-C_x^0\sin(k_{x0}x)\right]\left[-C_y^0\sin(k_{y0}y)\right]A_z^0 e^{-\gamma_z z} \tag{I18}$$

2-4-2.1 Case One: Symmetric Even LSE^x Mode i.e. $D_x^0 = 0$ in (I17)

With $D_x^0 = 0$, equation (I11) yields: $\dfrac{\mu_0 \cos(k_{x0}a)}{k_{x0}\sin(k_{x0}a)} = \dfrac{\mu_d \tan\left[k_{xd}^{(1)}d\right]}{k_{xd}^{(1)}}$

Equivalently, upon inverting: $\dfrac{k_{x0}}{\mu_0}\tan(k_{x0}a) = \dfrac{k_{xd}^{(1)}}{\mu_d}\cot\left[k_{xd}^{(1)}d\right]$ 　　　　(I-ES1)

where

$k_{x0} = \sqrt{k_0^2 - k_{y0}^2 + \gamma_z^2} = \sqrt{\omega^2 \mu_0 \varepsilon_0 - k_{y0}^2 + \gamma_z^2}$ which is from (IA2bi) for generally lossy

case

and $k_{x0} = \sqrt{k_0^2 - k_{y0}^2 - k_z^2} = \sqrt{\omega^2 \mu_0 \varepsilon_0 - k_{y0}^2 - k_z^2}$ which is from (IA2bii) for lossless case

also $k_{xd}^{(1)} = k_{xd}^{(2)} = \sqrt{k_d^2 - \left[k_{yd}^{(1)}\right]^2 + \gamma_z^2} = \sqrt{k_d^2 - \left[k_{yd}^{(2)}\right]^2 + \gamma_z^2} = \sqrt{\omega^2 \mu_d \varepsilon_d - k_{y0}^2 + \gamma_z^2}$

which is from (IB1bi) for generally lossy case,

and $k_{xd}^{(1)} = k_{xd}^{(2)} = \sqrt{k_d^2 - \left[k_{yd}^{(1)}\right]^2 - k_z^2} = \sqrt{\omega^2 \mu_d \varepsilon_d - k_{y0}^2 - k_z^2}$

which is from (IB1bii) for lossless case

where $k_{y0} = k_{yd}^{(1)} = k_{yd}^{(2)} = \dfrac{n\pi}{h}$

Therefore, for a certain frequency $f = \omega / (2\pi)$, and for a particular n^{th} mode

(corresponding to $k_{y0} = k_{yd}^{(1)} = k_{yd}^{(2)} = \dfrac{n\pi}{h}$ and a certain γ_{zn}), the above dispersion

equation (I-ES1) may be explicitly expressed as:

$$\dfrac{\sqrt{\omega^2 \mu_0 \varepsilon_0 - \left(\dfrac{n\pi}{h}\right)^2 + \gamma_{zn}^2}}{\mu_0} \tan\left[a\sqrt{\omega^2 \mu_0 \varepsilon_0 - \left(\dfrac{n\pi}{h}\right)^2 + \gamma_{zn}^2}\right] =$$

$$= \dfrac{\sqrt{\omega^2 \mu_d \varepsilon_d - \left(\dfrac{n\pi}{h}\right)^2 + \gamma_{zn}^2}}{\mu_d} \cot\left[d\sqrt{\omega^2 \mu_d \varepsilon_d - \left(\dfrac{n\pi}{h}\right)^2 + \gamma_{zn}^2}\right]$$ 　　　(I-ES2)

whose only unknown is γ_{zn}, [for a certain n^{th} mode and at a specific frequency $f = \omega\!\!\big/\!\!(2\pi)$], which can then be solved for numerically.

This solved γ_{zn}, together with $k_{y0} = \dfrac{n\pi}{h}$, can then be substituted into above equations for k_{xd} to obtain k_{x0} and $k_{xd}^{(1)} = k_{xd}^{(2)}$.

It is noted that ε_d may be expressed as $\varepsilon_d = \varepsilon_{rd}^{complex}\varepsilon_0$, with $\varepsilon_{rd}^{complex} = \varepsilon_{rd} - j\varepsilon_{rd}^{"}$

With $D_x^0 = 0$, equation (I12) yields $\dfrac{\mu_0 \cos\left(k_{x0}a\right)}{k_{x0}\sin\left(k_{x0}a\right)} = \dfrac{\mu_d \tan\left[k_{xd}^{(2)}d\right]}{k_{xd}^{(2)}d}$

Equivalently, upon inverting: $\dfrac{k_{x0}}{\mu_0}\tan\left(k_{x0}a\right) = \dfrac{k_{xd}^{(2)}}{\mu_d}\cot\left[k_{xd}^{(2)}d\right]$ (I-ES3)

Which is the same as (I-ES1) since $k_{xd}^{(1)} = k_{xd}^{(2)}$.

Therefore, (I12) also will result in the same dispersion characteristic equation as does (I11).

From (I4), with $D_x^0 = 0$, we have: $\dfrac{C_x^0 C_y^0 A_z^0}{\varepsilon_0}\cos\left(k_{x0}a\right) = \dfrac{D_x^{d1}C_y^{d1}A_z^{d1}}{\varepsilon_d}\sin\left[k_{xd}^{(1)}d\right]$

i.e. $\dfrac{D_x^{d1}C_y^{d1}A_z^{d1}}{C_x^0 C_y^0 A_z^0} = \dfrac{\varepsilon_d \cos\left(k_{x0}a\right)}{\varepsilon_0 \sin\left[k_{xd}^{(1)}d\right]}$ (I-ES4)

Normalizing by setting

$C_x^0 C_y^0 A_z^0 = 1$ (I-ES5)

Then (I-ES4) becomes

$D_x^{d1}C_y^{d1}A_z^{d1} = \dfrac{\varepsilon_d \cos\left(k_{x0}a\right)}{\varepsilon_0 \sin\left[k_{xd}^{(1)}d\right]}$ (I-ES6)

Also from (I5), with $D_x^0 = 0$, we have $-\dfrac{C_x^0 C_y^0 A_z^0}{\varepsilon_0}\cos(k_{x0}a) = \dfrac{D_x^{d2}C_y^{d2}A_z^{d2}}{\varepsilon_d}\sin\left[k_{xd}^{(2)}d\right]$

i.e. $\dfrac{D_x^{d2}C_y^{d2}A_z^{d2}}{C_x^0 C_y^0 A_z^0} = -\dfrac{\varepsilon_d\cos(k_{x0}a)}{\varepsilon_0\sin\left[k_{xd}^{(2)}d\right]}$ \hfill (I-ES7)

with $k_{xd}^{(1)} = k_{xd}^{(2)}$

As above, normalizing with (I-ES5), then (I-ES7) becomes:

$D_x^{d2}C_y^{d2}A_z^{d2} = -\dfrac{\varepsilon_d\cos(k_{x0}a)}{\varepsilon_0\sin\left[k_{xd}^{(2)}d\right]}$ \hfill (I-ES8)

Subsequently, using (I-ES5), (I-ES6) and (I-ES8), we can write expressions for all the electric and magnetic fields for this even symmetric LSE^x mode (with $D_x^0 = 0$) using equations (I1) through (I18). It is stressed that these field expressions pertain to one particular n^{th} mode corresponding to $k_{y0} = k_{yd}^{(1)} = k_{yd}^{(2)} = \dfrac{n\pi}{h}$ and a certain γ_{zn}, at a specific frequency $f = \dfrac{\omega}{2\pi}$. For each nth root γ_{zn} obtained from the dispersion equation (I-ES2), there corresponds to a certain set of phase constants, namely:

$k_{y0} = k_{yd}^{(1)} = k_{yd}^{(2)} = \dfrac{n\pi}{h}$

$k_{x0} = \sqrt{\omega^2\mu_0\varepsilon_0 - k_{y0}^2 + \gamma_{zn}^2}$

$k_{xd}^{(1)} = k_{xd}^{(2)} = \sqrt{k_d^2 - \left[k_{yd}^{(1)}\right]^2 + \gamma_{zn}^2} = \sqrt{k_d^2 - \left[k_{yd}^{(2)}\right]^2 + \gamma_{zn}^2} = \sqrt{\omega^2\mu_d\varepsilon_d - k_{y0}^2 + \gamma_{zn}^2}$

From (I1):

$E_z^0 = -\dfrac{k_{y0}}{\varepsilon_0}\cos(k_{x0}x)\sin(k_{y0}y)e^{-\gamma_{zn}z}$ \hfill (I-ES9)

From (I17):

$$E_y^0 = \frac{\gamma_z}{\varepsilon_0} \cos(k_{x0}x) \sin(k_{y0}y) e^{-\gamma_z z} \tag{I-ES10}$$

and

$$E_x^0 = 0 \quad (\text{since } \mathrm{LSE}^x \text{ mode}) \tag{I-ES11}$$

From (I6):

$$H_z^0 = \frac{k_{x0}\gamma_z}{j\omega\mu_0\varepsilon_0} \sin(k_{x0}x) \cos(k_{y0}y) e^{-\gamma_z z} \tag{I-ES12}$$

From (I18):

$$H_y^0 = \frac{k_{x0}k_{y0}}{j\omega\mu_0\varepsilon_0} \sin(k_{x0}x) \sin(k_{y0}y) e^{-\gamma_{zn} z} \tag{I-ES13}$$

Now, for LSE^x modes, we know that $H_x = \frac{1}{j\omega\mu_0\varepsilon_0}\left(\frac{\partial^2}{\partial x^2} + k^2\right)F_x$

Then using (IA1) with $D_y^0 = 0$ as well,

$$H_x^0 = \frac{1}{j\omega\mu_0\varepsilon_0}\left(\frac{\partial^2}{\partial x^2} + k_0^2\right)F_x^0 = \frac{1}{j\omega\mu_0\varepsilon_0}\left(-k_{x0}^2 + k_0^2\right)\cos(k_{x0}x)\cos(k_{y0}y)e^{-\gamma_{zn} z} \tag{I-ES14}$$

From (I2):

$$E_z^{d1} = -\frac{k_{yd}^{(1)}}{\varepsilon_d}\frac{\varepsilon_d \cos(k_{x0}a)}{\varepsilon_0 \sin\left[k_{xd}^{(1)}d\right]}\sin\left[k_{xd}^{(1)}(x+a+d)\right]\sin\left(k_{yd}^{(1)}y\right)e^{-\gamma_{zn} z} \tag{I-ES15}$$

From (I13):

$$E_y^{d1} = \frac{\gamma_{zn}}{\varepsilon_d}\frac{\varepsilon_d \cos(k_{x0}a)}{\varepsilon_0 \sin\left[k_{xd}^{(1)}d\right]}\sin\left[k_{xd}^{(1)}(x+a+d)\right]\cos\left(k_{yd}^{(1)}y\right)e^{-\gamma_{zn} z} \tag{I-ES16}$$

and

$$E_x^{d1} = 0 \quad (\text{since } \mathrm{LSE}^x \text{ mode}) \tag{I-ES17}$$

From (I7):

$$H_z^{d1} = -\frac{k_{xd}^{(1)}\gamma_z}{j\omega\mu_d\varepsilon_d}\frac{\varepsilon_d \cos(k_{x0}a)}{\varepsilon_0 \sin\left[k_{xd}^{(1)}d\right]}\cos\left[k_{xd}^{(1)}(x+a+d)\right]\cos\left(k_{yd}^{(1)}y\right)e^{-\gamma_{zn} z} \tag{I-ES18}$$

From (I14):

$$H_y^{d1} = -\frac{k_{xd}^{(1)} k_{yd}^{(1)}}{j\omega\mu_d\varepsilon_d} \frac{\varepsilon_d}{\varepsilon_0} \frac{\cos(k_{x0}a)}{\sin\left[k_{xd}^{(1)}d\right]} \cos\left[k_{xd}^{(1)}(x+a+d)\right] \sin\left(k_{yd}^{(1)}y\right) e^{-\gamma_{zn}z}$$ (I-ES19)

Using (IB1a), with its $C_x^{d1} = D_y^{d1} = 0$, we have

$$H_x^{d1} = \frac{1}{j\omega\mu_d\varepsilon_d}\left(\frac{\partial^2}{\partial x^2} + k_d^2\right)F_x^{d1} =$$

$$= \frac{k_d^2 - \left[k_{xd}^{(1)}\right]^2}{j\omega\mu_d\varepsilon_d} \frac{\varepsilon_d}{\varepsilon_0} \frac{\cos(k_{x0}a)}{\sin\left[k_{xd}^{(1)}\right]} \sin\left[k_{xd}^{(1)}(x+a+d)\right] \cos\left(k_{yd}^{(1)}y\right) e^{-\gamma_{zn}z}$$ (I-ES20)

From (I3):

$$E_z^{d2} = -\frac{k_{yd}^{(2)}}{\varepsilon_d}\left\{-\frac{\varepsilon_d}{\varepsilon_0}\frac{\cos(k_{x0}a)}{\sin\left[k_{xd}^{(2)}d\right]}\right\} \sin\left[k_{xd}^{(2)}(x-a-d)\right]\sin\left(k_{yd}^{(2)}y\right) e^{-\gamma_{zn}z} =$$

$$= \frac{k_{yd}^{(2)}}{\varepsilon_0} \frac{\cos(k_{x0}a)}{\sin\left[k_{xd}^{(2)}d\right]} \sin\left[k_{xd}^{(2)}(x-a-d)\right]\sin\left(k_{yd}^{(2)}y\right) e^{-\gamma_{zn}z}$$ (I-ES21)

From (I15):

$$E_y^{d2} = \frac{\gamma_z}{\varepsilon_d}\left\{-\frac{\varepsilon_d}{\varepsilon_0}\frac{\cos(k_{x0}a)}{\sin\left[k_{xd}^{(2)}d\right]}\right\} \sin\left[k_{xd}^{(2)}(x-a-d)\right]\cos\left(k_{yd}^{(2)}y\right) e^{-\gamma_{zn}z} =$$

$$= -\frac{\gamma_z}{\varepsilon_0} \frac{\cos(k_{x0}a)}{\sin\left[k_{xd}^{(2)}d\right]} \sin\left[k_{xd}^{(2)}(x-a-d)\right]\cos\left(k_{yd}^{(2)}y\right) e^{-\gamma_{zn}z}$$ (I-ES22)

and

$$E_x^{d2} = 0 \quad \text{(since LSE}^x \text{ mode)}$$ (I-ES23)

From (I8):

$$H_z^{d2} = -\frac{k_{xd}^{(2)}\gamma_z}{j\omega\mu_d\varepsilon_d}\left\{-\frac{\varepsilon_d}{\varepsilon_0}\frac{\cos(k_{x0}a)}{\sin\left[k_{xd}^{(2)}d\right]}\right\} \cos\left[k_{xd}^{(2)}(x-a-d)\right]\cos\left(k_{yd}^{(2)}y\right) e^{-\gamma_{zn}z} =$$

$$= \frac{k_{xd}^{(2)}\gamma_z}{j\omega\mu_d\varepsilon_0} \frac{\cos(k_{x0}a)}{\sin\left[k_{xd}^{(2)}d\right]} \cos\left[k_{xd}^{(2)}(x-a-d)\right]\cos\left(k_{yd}^{(2)}y\right) e^{-\gamma_{zn}z}$$ (I-ES24)

From (I16):

$$H_y^{d2} = -\frac{k_{xd}^{(2)}k_{yd}^{(2)}}{j\omega\mu_d\varepsilon_d}\left\{-\frac{\varepsilon_d\cos(k_{x0}a)}{\varepsilon_0\sin\left[k_{xd}^{(2)}d\right]}\right\}\cos\left[k_{xd}^{(2)}(x-a-d)\right]\sin\left(k_{yd}^{(2)}y\right)e^{-\gamma_{zn}z} =$$

$$= \frac{k_{xd}^{(2)}k_{yd}^{(2)}\cos(k_{x0}a)}{j\omega\mu_d\varepsilon_0\sin\left[k_{xd}^{(2)}d\right]}\cos\left[k_{xd}^{(2)}(x-a-d)\right]\sin\left(k_{yd}^{(2)}y\right)e^{-\gamma_{zn}z}$$

(I-ES25)

and finally using (IB2a) with its $C_x^{d2} = D_y^{d2} = 0$:

$$H_z^{d2} = \frac{1}{j\omega\mu_d\varepsilon_d}\left(\frac{\partial^2}{\partial x^2}+k_d^2\right)F_x^{d2} =$$

$$= \frac{k_d^2 - \left[k_{xd}^{(2)}\right]^2}{j\omega\mu_d\varepsilon_d}\left\{-\frac{\varepsilon_d\cos(k_{x0}a)}{\varepsilon_0\sin\left[k_{xd}^{(2)}d\right]}\right\}\sin\left[k_{xd}^{(2)}(x-a-d)\right]\cos\left(k_{yd}^{(2)}y\right)e^{-\gamma_{zn}z}$$

(I-ES26)

2-4-2.2 Case Two: Asymmetric Odd LSE^x Mode i.e. $C_x^0 = 0$ in (I17)

With $C_x^0 = 0$, equation (I11) yields:

$$-\frac{\mu_0\sin(k_{x0}a)}{k_{x0}\cos(k_{x0}a)} = \frac{\mu_d\tan\left[k_{xd}^{(1)}d\right]}{k_{xd}^{(1)}} \Rightarrow -\frac{\mu_0}{k_{x0}}\tan(k_{x0}a) = \frac{\mu_d\tan\left[k_{xd}^{(1)}d\right]}{k_{xd}^{(1)}}$$

Equivalently, upon inverting: $\dfrac{k_{x0}}{\mu_0}\cot(k_{x0}a) = -\dfrac{k_{xd}^{(1)}}{\mu_d}\cot\left[k_{xd}^{(1)}d\right]$ (I-OA1)

which can be explicitly expressed as:

$$\frac{\sqrt{\omega^2\mu_0\varepsilon_0 - \left(\frac{n\pi}{h}\right)^2 + \gamma_{zn}^2}}{\mu_0}\cot\left[a\sqrt{\omega^2\mu_0\varepsilon_0 - \left(\frac{n\pi}{h}\right)^2 + \gamma_{zn}^2}\right] =$$

$$= -\frac{\sqrt{\omega^2\mu_d\varepsilon_d - \left(\frac{n\pi}{h}\right)^2 + \gamma_{zn}^2}}{\mu_d}\cot\left[d\sqrt{\omega^2\mu_d\varepsilon_d - \left(\frac{n\pi}{h}\right)^2 + \gamma_{zn}^2}\right]$$

(I-OA2)

which, as before, whose only unknown is γ_{zn}, [for a certain n^{th} mode and at a specific

frequency $f = \omega/(2\pi)$], which can then be solved for numerically.

With $C_x^0 = 0$, equation (I12) yields:

$$-\frac{\mu_0 \sin(k_{x0}a)}{k_{x0}\cos(k_{x0}a)} = \frac{\mu_d \tan\left[k_{xd}^{(2)}d\right]}{k_{xd}^{(2)}} \Rightarrow -\frac{\mu_0}{k_{x0}}\tan(k_{x0}a) = \frac{\mu_d \tan\left[k_{xd}^{(2)}d\right]}{k_{xd}^{(2)}}$$

Equivalently, upon inverting: $\dfrac{k_{x0}}{\mu_0}\cot(k_{x0}a) = -\dfrac{k_{xd}^{(2)}}{\mu_d}\cot\left[k_{xd}^{(2)}d\right]$ (I-OA3)

which is the same as (I-OA1) since $k_{xd}^{(1)} = k_{xd}^{(2)}$.

Therefore, (I12) also will result in the same dispersion characteristic equation as does (I11).

From (I4), with $C_x^0 = 0$, we have $-\dfrac{D_x^0 C_y^0 A_z^0}{\varepsilon_0}\sin\left(k_{x0}a\right) = \dfrac{D_x^{d1} C_y^{d1} A_z^{d1}}{\varepsilon_d}\sin\left[k_{xd}^{(1)}d\right]$

i.e. $\dfrac{D_x^{d1} C_y^{d1} A_z^{d1}}{D_x^0 C_y^0 A_z^0} = -\dfrac{\varepsilon_d \sin\left(k_{x0}a\right)}{\varepsilon_0 \sin\left[k_{xd}^{(1)}d\right]}$ (I-OA4)

Normalizing by setting

$$D_x^0 C_y^0 A_z^0 = 1$$ (I-OA5)

then (I-OA4) becomes

$$D_x^{d1} C_y^{d1} A_z^{d1} = -\frac{\varepsilon_d \sin\left(k_{x0}a\right)}{\varepsilon_0 \sin\left[k_{xd}^{(1)}d\right]}$$ (I-OA6)

Also from (I5), with $C_x^0 = 0$, we have $-\dfrac{D_x^0 C_y^0 A_z^0}{\varepsilon_0}\sin\left(k_{x0}a\right) = \dfrac{D_x^{d2} C_y^{d2} A_z^{d2}}{\varepsilon_d}\sin\left[k_{xd}^{(2)}d\right]$

i.e. $\dfrac{D_x^{d2} C_y^{d2} A_z^{d2}}{D_x^0 C_y^0 A_z^0} = -\dfrac{\varepsilon_d \sin\left(k_{x0}a\right)}{\varepsilon_0 \sin\left[k_{xd}^{(2)}d\right]}$ (I-OA7)

with $k_{xd}^{(1)} = k_{xd}^{(2)}$.

As above, normalizing with (I-OA5), then (I-OA7) becomes:

$$D_x^{d2} C_y^{d2} A_z^{d2} = -\frac{\varepsilon_d \sin\left(k_{x0}a\right)}{\varepsilon_0 \sin\left[k_{xd}^{(2)}d\right]}$$ (I-OA8)

Subsequently, as before in the symmetric even case, using (I-OA5), (I-OA6) and (I-OA8), we can write expressions for all the electric and magnetic fields for this odd asymmetric LSE^x mode (with $C_x^0 = 0$) using equations (I1) through (I18).

From (I1):

$$E_z^0 = -\frac{k_{y0}}{\varepsilon_0} \sin(k_{x0}x) \sin(k_{y0}y) e^{-\gamma_{zn}z}$$

From (I17):

$$E_y^0 = \frac{\gamma_z}{\varepsilon_0} \sin(k_{x0}x) \cos(k_{y0}y) e^{-\gamma_{zn}z}$$

and

$$E_x^0 = 0 \quad (\text{since LSE}^x \text{ mode})$$

From (I6):

$$H_z^0 = -\frac{k_{x0}\gamma_z}{j\omega\mu_0\varepsilon_0} \cos(k_{x0}x) \cos(k_{y0}y) e^{-\gamma_{zn}z}$$

From (I18):

$$H_y^0 = -\frac{k_{x0}k_{y0}}{j\omega\mu_0\varepsilon_0} \cos(k_{x0}x) \sin(k_{y0}y) e^{-\gamma_{zn}z}$$

Now, for LSE^x modes, we know that $H_x = \frac{1}{j\omega\mu\varepsilon}\left(\frac{\partial^2}{\partial x^2} + k^2\right)F_x$

Then using (IA1) with $C_x^0 = D_y^0 = 0$ as well,

$$H_x^0 = \frac{1}{j\omega\mu_0\varepsilon_0}\left(\frac{\partial^2}{\partial x^2} + k_0^2\right)F_x^0 = \frac{1}{j\omega\mu_0\varepsilon_0}\left(-k_{x0}^2 + k_0^2\right)\sin(k_{x0}x)\cos(k_{y0}y)e^{-\gamma_{zn}z}$$

From (I2):

$$E_z^{d1} = -\frac{k_{yd}^{(1)}}{\varepsilon_d}\left\{-\frac{\varepsilon_d \cos(k_{x0}a)}{\varepsilon_0 \sin\left[k_{xd}^{(1)}d\right]}\right\}\sin\left[k_{xd}^{(1)}(x+a+d)\right]\sin\left(k_{yd}^{(1)}y\right)e^{-\gamma_{zn}z}$$

From (I13):

$$E_y^{d1} = -\frac{\gamma_{zn}}{\varepsilon_d}\frac{\varepsilon_d \sin(k_{x0}a)}{\varepsilon_0 \sin\left[k_{xd}^{(1)}d\right]}\sin\left[k_{xd}^{(1)}(x+a+d)\right]\cos\left(k_{yd}^{(1)}y\right)e^{-\gamma_{zn}z}$$

and

$$E_x^{d1} = 0 \quad \text{(since LSE}^x \text{ mode)}$$

From (I7):

$$H_z^{d1} = \frac{k_{xd}^{(1)}\gamma_z}{j\omega\mu_d\varepsilon_d}\frac{\varepsilon_d \sin(k_{x0}a)}{\varepsilon_0 \sin\left[k_{xd}^{(1)}d\right]}\cos\left[k_{xd}^{(1)}(x+a+d)\right]\cos\left(k_{yd}^{(1)}y\right)e^{-\gamma_{zn}z}$$

Using (IB1a), with its $C_x^{d2} = D_y^{d2} = 0$, we have

$$H_x^{d1} = \frac{1}{j\omega\mu_d\varepsilon_d}\left(\frac{\partial^2}{\partial x^2}+k_d^2\right)F_x^{d1} =$$

$$= \frac{k_d^2 - \left[k_{xd}^{(1)}\right]^2}{j\omega\mu_d\varepsilon_d}\left\{-\frac{\varepsilon_d \sin(k_{x0}a)}{\varepsilon_0 \sin\left[k_{xd}^{(1)}d\right]}\right\}\sin\left[k_{xd}^{(1)}(x+a+d)\right]\cos\left(k_{yd}^{(1)}y\right)e^{-\gamma_{zn}z}$$

From (I14):

$$H_y^{d1} = -\frac{k_{xd}^{(1)}k_{yd}^{(1)}}{j\omega\mu_d\varepsilon_d}\left\{-\frac{\varepsilon_d \sin(k_{x0}a)}{\varepsilon_0 \sin\left[k_{xd}^{(1)}d\right]}\right\}\cos\left[k_{xd}^{(1)}(x+a+d)\right]\sin\left(k_{yd}^{(1)}y\right)e^{-\gamma_{zn}z} =$$

$$= \frac{k_{xd}^{(1)}k_{yd}^{(1)}\sin(k_{x0}a)}{j\omega\mu_d\varepsilon_0 \sin\left[k_{xd}^{(1)}d\right]}\cos\left[k_{xd}^{(1)}(x+a+d)\right]\sin\left(k_{yd}^{(1)}y\right)e^{-\gamma_{zn}z}$$

From (I3):

$$E_z^{d2} = \frac{k_{yd}^{(2)}}{\varepsilon_d}\frac{\varepsilon_d \sin(k_{x0}a)}{\varepsilon_0 \sin\left[k_{xd}^{(2)}d\right]}\sin\left[k_{xd}^{(2)}(x-a-d)\right]\sin\left(k_{yd}^{(2)}y\right)e^{-\gamma_{zn}z} =$$

$$= \frac{k_{yd}^{(2)}\sin(k_{x0}a)}{\varepsilon_0 \sin\left[k_{xd}^{(2)}d\right]}\sin\left[k_{xd}^{(2)}(x-a-d)\right]\sin\left(k_{yd}^{(2)}y\right)e^{-\gamma_{zn}z}$$

From (I15):

$$E_y^{d2} = -\frac{\gamma_z}{\varepsilon_d}\frac{\varepsilon_d \sin(k_{x0}a)}{\varepsilon_0 \sin\left[k_{xd}^{(2)}d\right]}\sin\left[k_{xd}^{(2)}(x-a-d)\right]\cos\left(k_{yd}^{(2)}y\right)e^{-\gamma_{zn}z} =$$

$$= -\frac{\gamma_z \sin(k_{x0}a)}{\varepsilon_0 \sin\left[k_{xd}^{(2)}d\right]}\sin\left[k_{xd}^{(2)}(x-a-d)\right]\cos\left(k_{yd}^{(2)}y\right)e^{-\gamma_{zn}z}$$

and

$E_x^{d2} = 0$ (since LSE^x mode)

From (I8):

$$H_z^{d2} = \frac{k_{xd}^{(2)}\gamma_z}{j\omega\mu_d\varepsilon_d} \frac{\varepsilon_d \sin(k_{x0}a)}{\varepsilon_0 \sin[k_{xd}^{(2)}d]} \cos\left[k_{xd}^{(2)}(x-a-d)\right]\cos\left(k_{yd}^{(2)}y\right)e^{-\gamma_{zn}z} =$$

$$= \frac{k_{xd}^{(2)}\gamma_z \sin(k_{x0}a)}{j\omega\mu_d\varepsilon_0 \sin[k_{xd}^{(2)}d]} \cos\left[k_{xd}^{(2)}(x-a-d)\right]\cos\left(k_{yd}^{(2)}y\right)e^{-\gamma_{zn}z}$$

From (I16):

$$H_y^{d2} = \frac{k_{xd}^{(2)}k_{yd}^{(2)}}{j\omega\mu_d\varepsilon_d} \frac{\varepsilon_d \sin(k_{x0}a)}{\varepsilon_0 \sin[k_{xd}^{(2)}d]} \cos\left[k_{xd}^{(2)}(x-a-d)\right]\sin\left(k_{yd}^{(2)}y\right)e^{-\gamma_{zn}z} =$$

$$= \frac{k_{xd}^{(2)}k_{yd}^{(2)} \sin(k_{x0}a)}{j\omega\mu_d\varepsilon_0 \sin[k_{xd}^{(2)}d]} \cos\left[k_{xd}^{(2)}(x-a-d)\right]\sin\left(k_{yd}^{(2)}y\right)e^{-\gamma_{zn}z}$$

and finally using (IB2a) with its $C_x^{d2} = D_y^{d2} = 0$:

$$H_x^{d2} = \frac{1}{j\omega\mu_d\varepsilon_d}\left(\frac{\partial^2}{\partial x^2} + k_d^2\right)F_x^{d2} =$$

$$= \frac{k_d^2 - \left[k_{xd}^{(2)}\right]^2}{j\omega\mu_d\varepsilon_d}\left\{-\frac{\varepsilon_d \sin(k_{x0}a)}{\varepsilon_0 \sin[k_{xd}^{(2)}d]}\right\}\sin\left[k_{xd}^{(2)}(x-a-d)\right]\cos\left(k_{yd}^{(2)}y\right)e^{-\gamma_{zn}z}$$

2-4-3 **Case (II): LSM^x or TM^x mode** (with x direction normal to discontinuity interface)

(A) For central freespace region: $-a \le x \le a$: superscript or subscript '0'

$$A_x^0(-a \le x \le a, y, z) = \left[C_x^0 \cos(k_{x0}x) + D_x^0 \sin(k_{x0}x)\right]\left[C_y^0 \cos(k_{y0}y) + D_y^0 \sin(k_{y0}y)\right]A_z^0 e^{-\gamma_z z}$$

(IIA1)

(B) For dielectric region: $-(a+d) \le x \le a$ and $a < x < a+d$

(1) Left dielectric region: $-(a+d) \leq x \leq a$ (superscript or subscript '1')

$$A_x^{d1}[-(a+d) \leq x \leq -a, y, z] = \left\{ C_x^{d1} \cos\left[k_{xd}^{(1)}(x+a+d) \right] + D_x^{d1} \sin\left[k_{xd}^{(1)}(x+a+d) \right] \right\}$$

$$\times \left\{ C_y^{d1} \cos\left[k_{yd}^{(1)} y \right] + D_y^{d1} \sin\left[k_{yd}^{(1)} y \right] \right\} A_z^{d1} e^{-\gamma_z z} \qquad \text{(IIB1a)}$$

(2) Right dielectric region: $a \leq x \leq a+d$ (superscript or subscript '2')

$$A_x^{d2}[a \leq x \leq a+d, y, z] = \left\{ C_x^{d2} \cos\left[k_{xd}^{(2)}(x-a-d) \right] + D_x^{d2} \sin\left[k_{xd}^{(2)}(x-a-d) \right] \right\} \quad \text{(IIB2a)}$$

Here, LSM^x and LSE^x have many formulas in common, except some equations. Table I below shows the difference in those two cases. We will omit the boundary conditions and some equations that are the same with LSE cases.

LSE	LSM
$C_x^{d1(d2)} = 0$	$D_x^{d1(d2)} = 0$
$D_y^{0(d2)} = 0$	$C_y^{0(d2)} = 0$
$E_x = 0$	$E_x = \dfrac{1}{j\omega\mu\varepsilon}\left(\dfrac{\partial^2}{\partial x^2} + k^2 \right) A_x$
$E_y = -\dfrac{1}{\varepsilon}\dfrac{\partial F_x}{\partial z}$	$E_y = \dfrac{1}{j\omega\mu\varepsilon}\dfrac{\partial^2 A_x}{\partial x \partial y}$
$E_z = \dfrac{1}{\varepsilon}\dfrac{\partial F_x}{\partial y}$	$E_z = \dfrac{1}{j\omega\mu\varepsilon}\dfrac{\partial^2 A_x}{\partial x \partial z}$
$H_x = \dfrac{1}{j\omega\mu_0\varepsilon_0}\left(\dfrac{\partial^2}{\partial x^2} + k^2 \right) F_x$	$H_x = 0$
$H_y = \dfrac{1}{j\omega\mu\varepsilon}\dfrac{\partial^2 F_x}{\partial x \partial y}$	$H_y = \dfrac{1}{\mu}\dfrac{\partial A_x}{\partial z}$
$H_z = \dfrac{1}{j\omega\mu\varepsilon}\dfrac{\partial^2 F_x}{\partial x \partial z}$	$H_z = -\dfrac{1}{\mu}\dfrac{\partial A_x}{\partial y}$

Table I. The comparison of the electromagnetic distribution between LSE and LSM

2-4-3.1 Case One: Symmetric Even LSM$^{\mathbf{x}}$ Mode i.e. $D_x^0 = 0$ in (II13)

With $D_x^0 = 0$, equation (II11) yields: $\dfrac{k_{x0}\sin(k_{x0}a)}{\varepsilon_0\cos(k_{x0}a)} = -\dfrac{k_{xd}^{(1)}\tan\left[k_{xd}^{(1)}d\right]}{\varepsilon_d}$

i.e. $\dfrac{k_{x0}}{\varepsilon_0}\tan(k_{x0}a) = -\dfrac{k_{xd}^{(1)}}{\varepsilon_d}\tan\left[k_{xd}^{(1)}d\right]$ (II-ES1)

which can be explicitly expressed as:

$$\frac{\sqrt{\omega^2\mu_0\varepsilon_0 - \left(\dfrac{n\pi}{h}\right)^2 + \gamma_{zn}^2}}{\varepsilon_0}\tan\left[a\sqrt{\omega^2\mu_0\varepsilon_0 - \left(\frac{n\pi}{h}\right)^2 + \gamma_{zn}^2}\right] =$$

$$= -\frac{\sqrt{\omega^2\mu_d\varepsilon_d - \left(\dfrac{n\pi}{h}\right)^2 + \gamma_{zn}^2}}{\varepsilon_d}\tan\left[d\sqrt{\omega^2\mu_d\varepsilon_d - \left(\frac{n\pi}{h}\right)^2 + \gamma_{zn}^2}\right] \quad \text{(II-ES2)}$$

which, as before, whose only unknown is γ_{zn}, [for a certain n^{th} mode and at a specific

frequency $f = \omega/(2\pi)$], which can then be solved for numerically.

With $D_x^0 = 0$, equation (II12) yields: $\dfrac{k_{x0}}{\varepsilon_0}\tan(k_{x0}a) = -\dfrac{k_{xd}^{(2)}}{\varepsilon_d}\tan\left[k_{xd}^{(2)}d\right]$ (II-ES3)

which is the same as (II-ES1) since $k_{xd}^{(1)} = k_{xd}^{(2)}$.

Therefore, (II12) also will result in the same dispersion characteristic equation as does

(II11).

2-4-3.2 Case Two: Asymmetric Odd LSM$^{\mathbf{x}}$ Mode i.e. $C_x^0 = 0$ in (II13)

With $C_x^0 = 0$, equation (I11) yields:

$$-\frac{k_{x0}\cos(k_{x0}a)}{\varepsilon_0 \sin(k_{x0}a)} = -\frac{k_{xd}^{(1)}\tan\left[k_{xd}^{(1)}d\right]}{\varepsilon_d} \Rightarrow \frac{k_{x0}}{\varepsilon_0}\cot\left(k_{x0}a\right) = \frac{k_{xd}^{(1)}}{\varepsilon_d}\tan\left[k_{xd}^{(1)}d\right]$$

Therefore, we have: $\dfrac{k_{x0}}{\varepsilon_0}\cot\left(k_{x0}a\right) = \dfrac{k_{xd}^{(1)}}{\varepsilon_d}\tan\left[k_{xd}^{(1)}d\right]$ (II-OA1)

where

$$k_{x0} = \sqrt{k_0^2 - k_{y0}^2 + \gamma_z^2} = \sqrt{\omega^2 \mu_0 \varepsilon_0 - k_{y0}^2 + \gamma_z^2}$$

which is from (IIA2bi) for generally lossy case

also

$$k_{xd}^{(1)} = k_{xd}^{(2)} = \sqrt{k_d^2 - \left[k_{yd}^{(1)}\right]^2 + \gamma_z^2} = \sqrt{k_d^2 - \left[k_{yd}^{(2)}\right]^2 + \gamma_z^2} = \sqrt{\omega^2 \mu_d \varepsilon_d - k_{y0}^2 + \gamma_z^2}$$

which is from (IIB1bii) for lossless case

where

$$k_{y0} = k_{yd}^{(1)} = k_{yd}^{(2)} = \frac{n\pi}{h}$$

Therefore, for a certain frequency $f = \omega/(2\pi)$, and for a particular n^{th} mode (corresponding to $k_{y0} = k_{yd}^{(1)} = k_{yd}^{(2)} = \frac{n\pi}{h}$ and a certain γ_{zn}), the above dispersion equation (II-OA1) may be explicitly expressed as:

$$\frac{\sqrt{\omega^2 \mu_0 \varepsilon_0 - \left(\frac{n\pi}{h}\right)^2 + \gamma_{zn}^2}}{\varepsilon_0}\cot\left[a\sqrt{\omega^2 \mu_0 \varepsilon_0 - \left(\frac{n\pi}{h}\right)^2 + \gamma_{zn}^2}\right] =$$

$$= \frac{\sqrt{\omega^2 \mu_d \varepsilon_d - \left(\frac{n\pi}{h}\right)^2 + \gamma_{zn}^2}}{\varepsilon_d}\tan\left[d\sqrt{\omega^2 \mu_d \varepsilon_d - \left(\frac{n\pi}{h}\right)^2 + \gamma_{zn}^2}\right]$$ (II-OA2)

which, as before, whose only unknown is γ_{zn}, [for a certain n^{th} mode and at a specific

frequency $f = \omega/(2\pi)$], which can then be solved for numerically.

This solved γ_{zn}, together with $k_{y0} = \dfrac{n\pi}{h}$, can then be substituted into above equations

for k_{x0} and k_{xd} to obtain k_{x0} and $k_{xd}^{(1)} = k_{xd}^{(2)}$.

It is noted that ε_d may be expressed as $\varepsilon_d = \varepsilon_{rd}^{complex}\varepsilon_0$, with $\varepsilon_{rd}^{complex} = \varepsilon_{rd} - j\varepsilon_{rd}^{"}$

With $C_x^0 = 0$, equation (II12) yields:

$$\frac{k_{x0}}{\varepsilon_0}\cot(k_{x0}a) = \frac{k_{xd}^{(2)}}{\varepsilon_d}\tan\left[k_{xd}^{(2)}d\right] \tag{II-OA3}$$

which is the same as (II-OA1) since $k_{xd}^{(1)} = k_{xd}^{(2)}$.

Therefore, (II12) also will result in the same dispersion characteristic equation as does (II11).

2-5 The characteristic equations after modification

From above, TEM-x solution in mathematically stated,

$$k_{xd}^{(1)} = k_{xd}^{(2)} = k_d = \omega\sqrt{\mu_d\varepsilon_d} \tag{Eq-18}$$

Note that (IB1a), with (1) above taken into effect. This gives the form

$$F_x^{d1}[-(a+d) < x < -a, y, z] = \left\{ C_x^{d1}\cos[\overset{k_{xd}^{(1)}}{k_d}(x+a+d)] + D_x^{d1}\sin[\overset{k_{xd}^{(1)}}{k_d}(x+a+d)] \right\}\cdots$$

$$\cdots \times \left\{ C_y^{d1}\cos\left[k_{yd}^{(1)}y\right] + D_y^{d1}\sin\left[k_{yd}^{(1)}y\right] \right\} A_z^{d1}e^{-\gamma_z z}$$

$$\tag{Eq-19}$$

As such, Case 2 of the solution to Example 6-1 in Balanis Advanced Engineering Electromagnetics (AEE) [8] on Pg 263 pertaining to TEM-x mode (with z and x swapped there) can be invoked here. This (Eq-19) indeed coheres with the second equation on Pg 264 Balanis AEE, being

$$H_x = \frac{1}{j\omega\mu_d\varepsilon_d}\left(\frac{\partial}{\partial x^2} + \omega^2\mu_d\varepsilon_d\right)F_x^{d1} \equiv 0,$$
(Eq-20)

along with the null E_x that is already in place. Note no matter what the TEM-x solution being stated at the bottom of page 263 in Balanis AEE, i.e. $\partial/\partial z \neq 0$, $\partial/\partial y \neq 0$ actually holds here, even though it's being invalid for ordinary homogeneous media (this pin-lattice medium here however is unusual and not subjected to that invalidity). That is to say, the γ_z of (Eq-19) above remain nonzero in the analysis. Also, it is remained of the case in the center region of the waveguide where has no pins.

However, although the γ_z in the pin-lattice-embedded slab region must be nonzero, and equal to the center region for phase continuity, it doesn't mean that there would be aactually wave propagation in that host region with a component along the waveguide z axis. On the contrary, the TEM-x waves propagate along the pins (x-direction) within an increasing part of the host medium between neighboring infinitesimally-separated pins acting as a transmission line. In more properly words, they are standing waves on the shorted (PEC wall) transmission line rather than propagate waves. Seeing the trigonometric functional forms of (Eq-19) for the variation with x, they are slightly out of phase from those in neighboring transmission-line regions such that the phase progressively along y and z (tangential to the slab surface) follow those in the center part of the waveguide. In an asymptotic sense then, $k_{yd}^{(1\&2)}$ and γ_z in the lattice-layers are being as nonzero in the analysis. As a result, the usual $\left[k_{xd}^{(1\&2)}\right]^2 + \left[k_{yd}^{(1\&2)}\right]^2 - \gamma_z^2 = k_d^2$ no longer holds here. This formula is valid only for the ordinary media within which actual waves propagate along a direction with x, y and z components.

The pin-lattice sidewall of the waveguide supports TEM-*x* waves along *x* only, but no waves actually propagate obliquely with components along *z* or *y*.

Therefore, the new characteristic equations for the four mode categories: LSE Symmetric, LSE Asymmetric, LSM Symmetric, and LSM Asymmetric are now:

(i). LSE Symmetric:

$$\frac{\sqrt{\omega^2 \mu_0 \varepsilon_0 - \left(n\pi/h\right)^2 + \gamma_{z_n}^2}}{\mu_0} \tan\left[a\sqrt{\omega^2 \mu_0 \varepsilon_0 - \left(n\pi/h\right)^2 + \gamma_{z_n}^2}\right] = \frac{\omega\sqrt{\mu_d \varepsilon_d}}{\mu_d} \cot\left(\omega d \sqrt{\mu_d \varepsilon_d}\right)$$

(Eq-21)

(ii). LSE Asymmetric:

$$\frac{\sqrt{\omega^2 \mu_0 \varepsilon_0 - \left(n\pi/h\right)^2 + \gamma_{z_n}^2}}{\mu_0} \cot\left[a\sqrt{\omega^2 \mu_0 \varepsilon_0 - \left(n\pi/h\right)^2 + \gamma_{z_n}^2}\right] = -\frac{\omega\sqrt{\mu_d \varepsilon_d}}{\mu_d} \cot\left(\omega d \sqrt{\mu_d \varepsilon_d}\right)$$

(Eq-22)

(iii). LSM Symmetric:

$$\frac{\sqrt{\omega^2 \mu_0 \varepsilon_0 - \left(n\pi/h\right)^2 + \gamma_{z_n}^2}}{\varepsilon_0} \tan\left[a\sqrt{\omega^2 \mu_0 \varepsilon_0 - \left(n\pi/h\right)^2 + \gamma_{z_n}^2}\right] = -\frac{\omega\sqrt{\mu_d \varepsilon_d}}{\varepsilon_d} \tan\left(\omega d \sqrt{\mu_d \varepsilon_d}\right)$$

(Eq-23)

(iv). LSM Asymmetric:

$$\frac{\sqrt{\omega^2 \mu_0 \varepsilon_0 - \left(n\pi/h\right)^2 + \gamma_{z_n}^2}}{\varepsilon_0} \cot\left[a\sqrt{\omega^2 \mu_0 \varepsilon_0 - \left(n\pi/h\right)^2 + \gamma_{z_n}^2}\right] = \frac{\omega\sqrt{\mu_d \varepsilon_d}}{\varepsilon_d} \tan\left(\omega d \sqrt{\mu_d \varepsilon_d}\right)$$

(Eq-24)

where h is the height along y, a is half the central width along x, and d is the slab

thickness.

III. Discussion

3-1 Initial setting of dimension - width: 20 mm & height: 5 mm

At first, we choose a waveguide with dimensions: 5 mm in height and 20 mm in width.

Fig. 8 below shows the perfect agreement with HFSS simulation result and CST simulation result. Both make use of waveport modes for the simulation. Orange stars represent HFSS, and the blue spades represent CST simulation.

By this figure, it is found that there would be modes excited at about frequency 7 GHz, 14 GHz, 18 GHz, 22~23 GHz, and 25GHz.
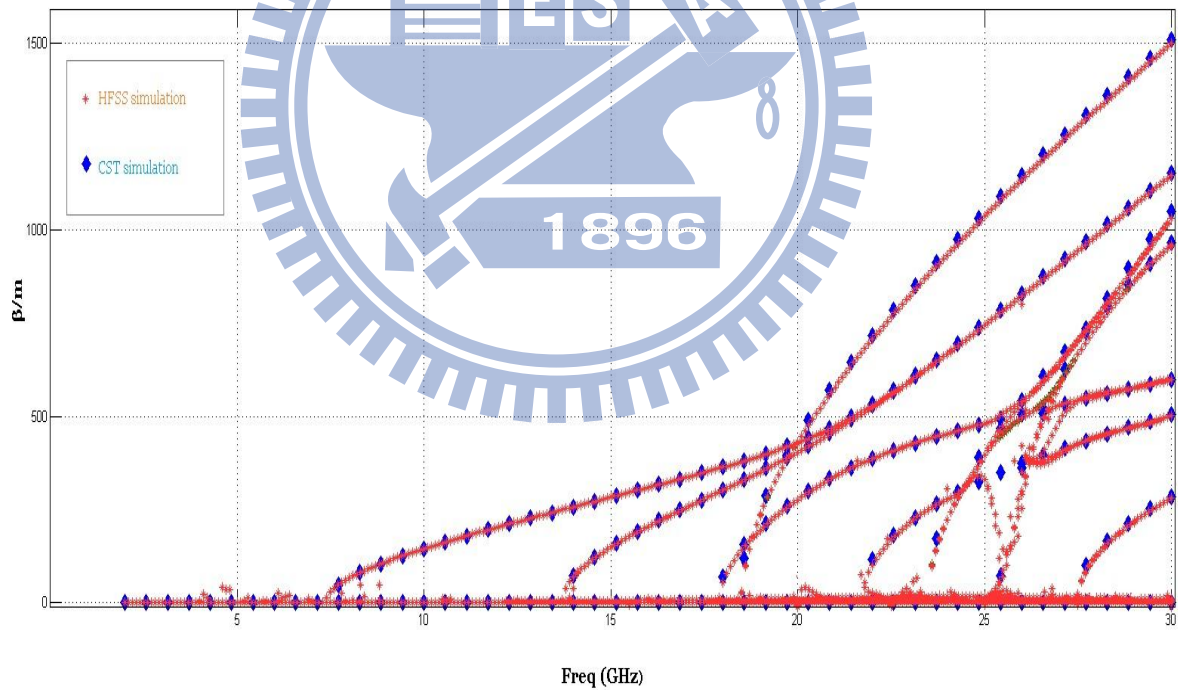
Fig.8　Simulation results of the comparison of CST and HFSS

At first, we choose the waveguide with the dimension 5 mm height, 20 mm width.

Use above characteristic equations and simulated by MATLAB, and then compared with HFSS simulation result. The comparison is shown as below.
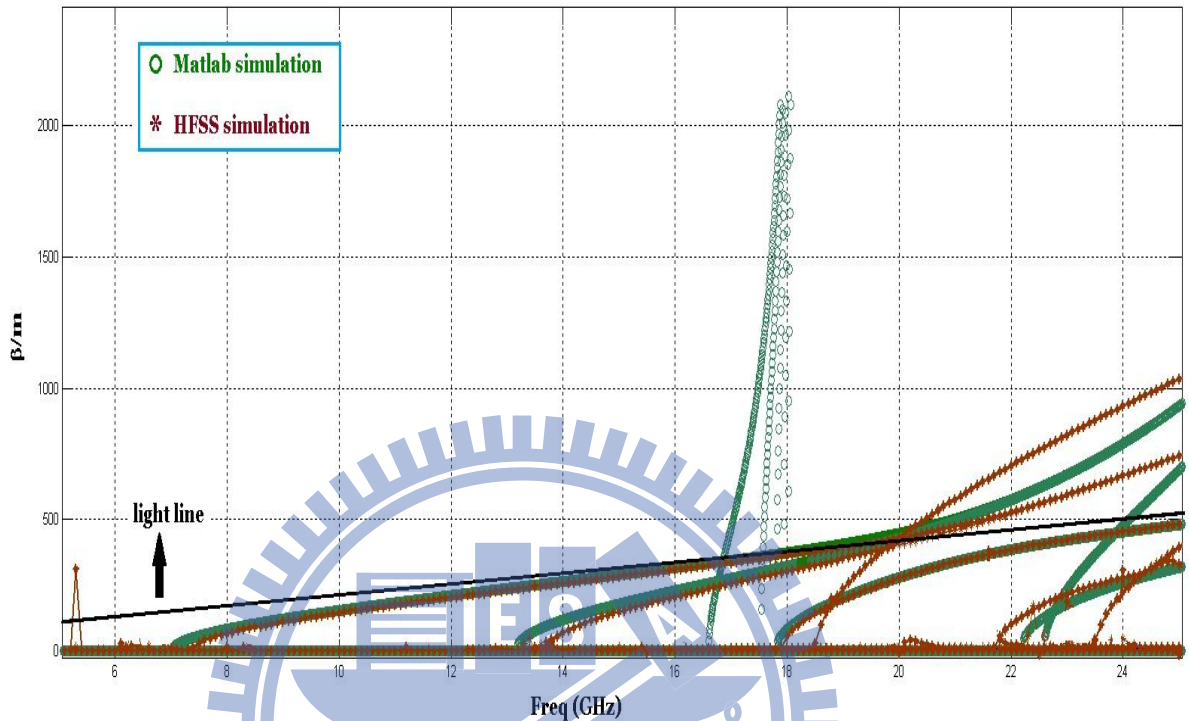

Fig.9   Simulation results of the comparison of MATLAB and HFSS

From the above results, fine agreement between the different simulation tools is observed, verifying the accuracy of the waveport mode simulation setting. However, even though this dimension has more obvious effects that we want to see, it still has difficulties with the measure processing for the not fitting adaptor. This way, we tried another dimension with double height that is 10 mm, and the same width 20mm.

The next section, we will go through the introduction of new dimension.

3-2 Final setting of dimension - width: 20 mm & height: 10 mm

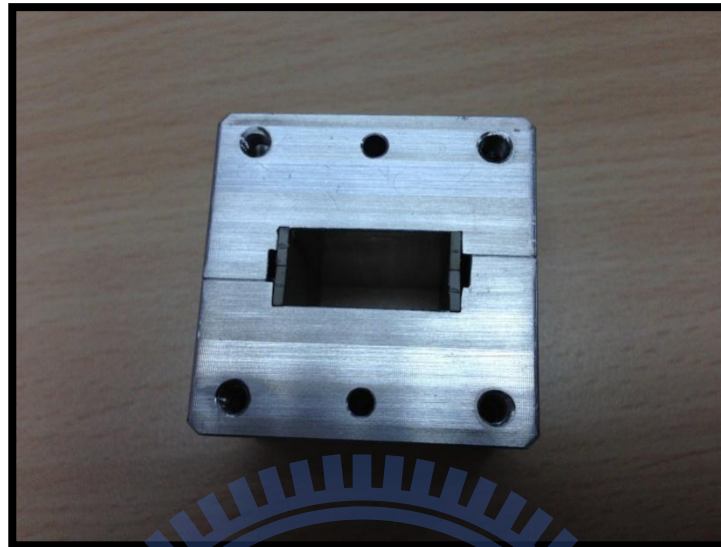**3-2-1 The pictures of the finished manufacture**

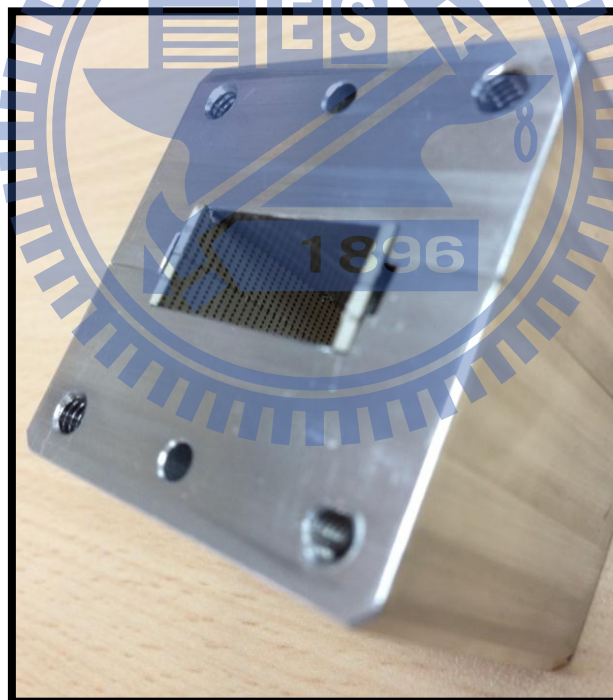Fig.10(a) Front sight of the sidewall-dielectric waveguide

Fig.10(b) Side sight of the sidewall-dielectric waveguide

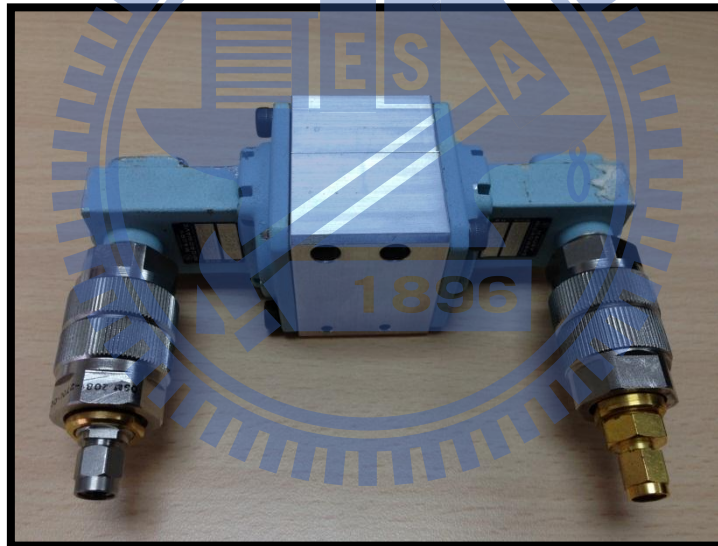Fig.10(c) The front sight of WR90 adaptor

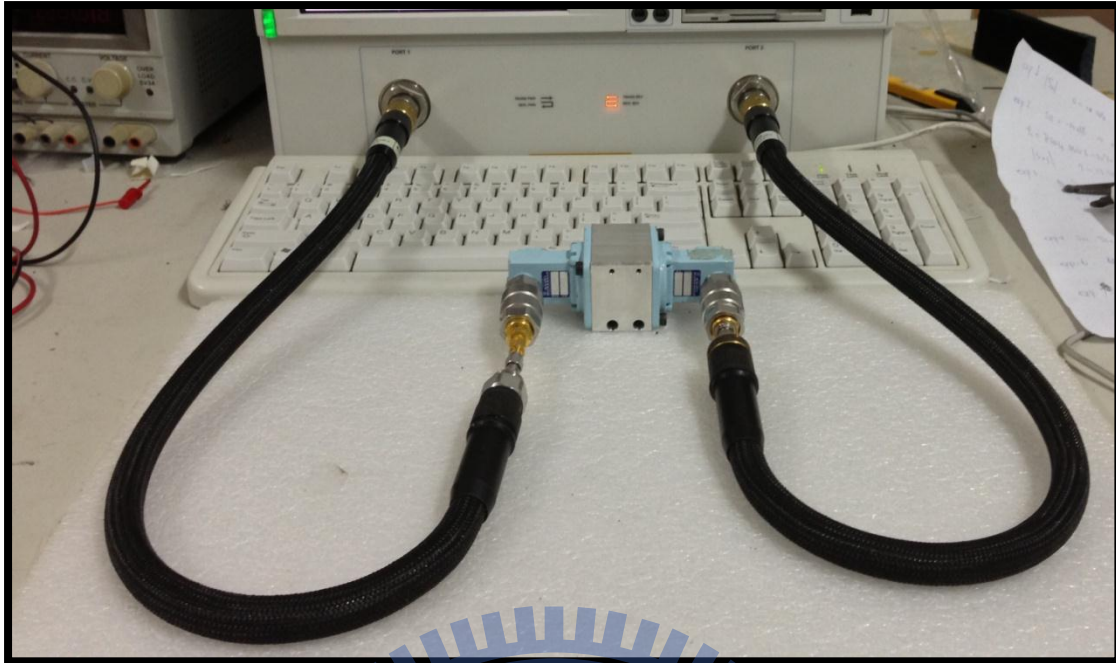Fig.10(d) The waveguide connected with the adaptor

Fig. 10(e) The setting of the measurement

3-2-2 The comparison of the S-parameter by simulated and measured

Fig.11 below shows the results by simulated and measured. Red spades represents the HFSS simulation result and the blue star represents the measurement.

However, this diagram cannot show the characteristic of the stop-band obviously. This way, it won't able to show our objective to create the sidewall-loaded waveguide in this dimension
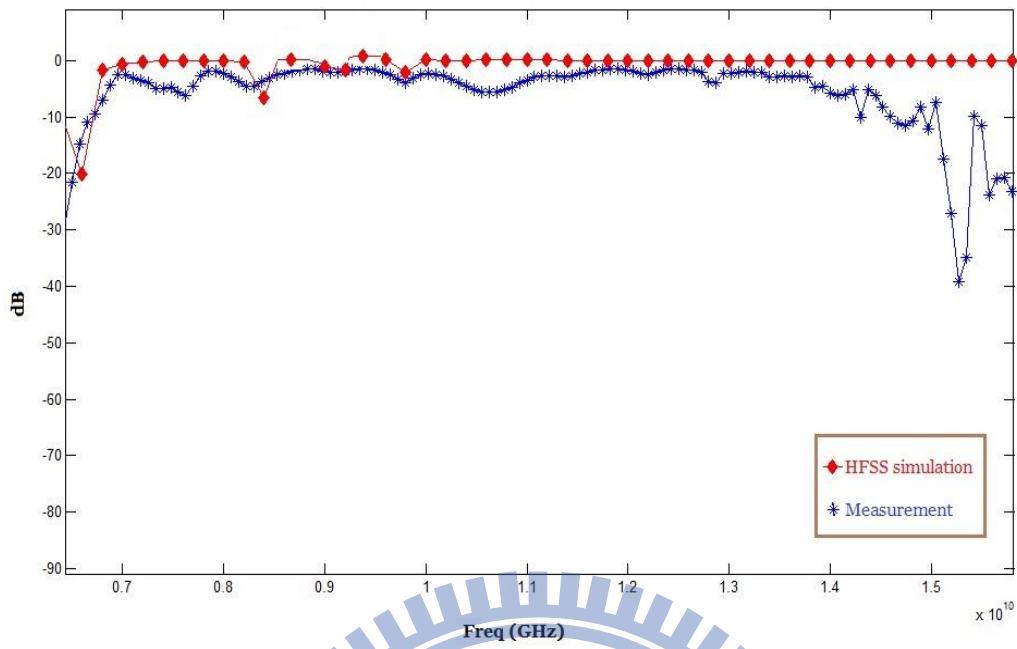
Fig.11   The comparison of the simulation and measurement

Fig.12 represents the eigenmode simulation of Rogers-3010 substrate, the sidewall

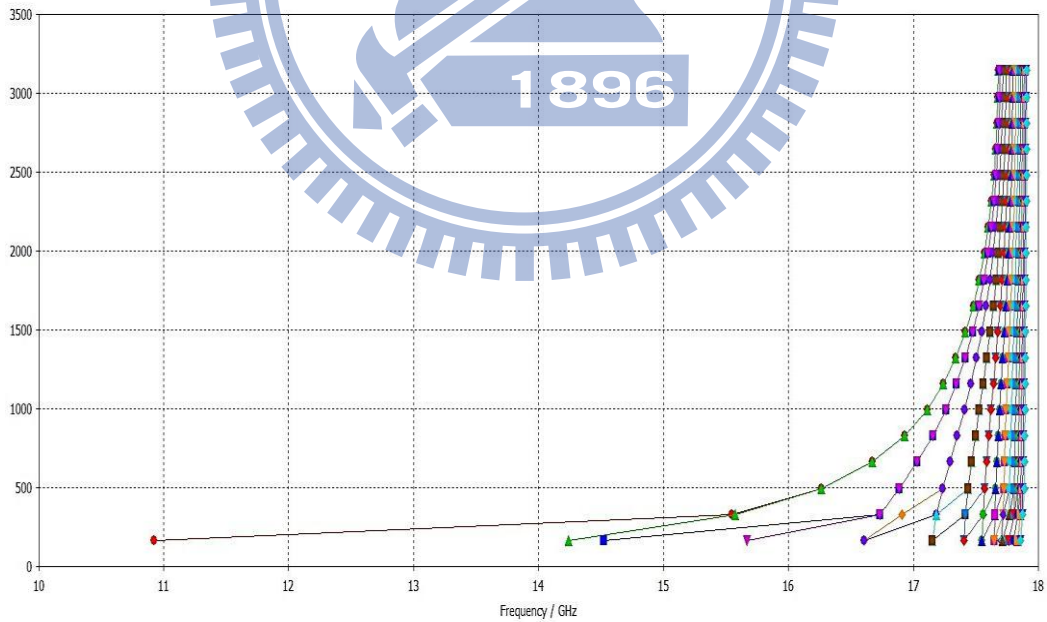width is 1.28 mm, and there has no stop-band.

Fig.12 CST eigenmode simulation of RO-3010 substrate

3-2-3 The CST simulation of the Styrofoam substrate

Because the material we've chosen doesn't show good, obvious stop-band in the dispersion diagram by CST simulation. We try to find another dimension with another material to reveal the stop-band, which may apply to the waveguide filter, and we will discuss about it in the next part. Fig.13 below shows the obvious stop-band between ten Giga-Hertz to seventeen Giga-Hertz.
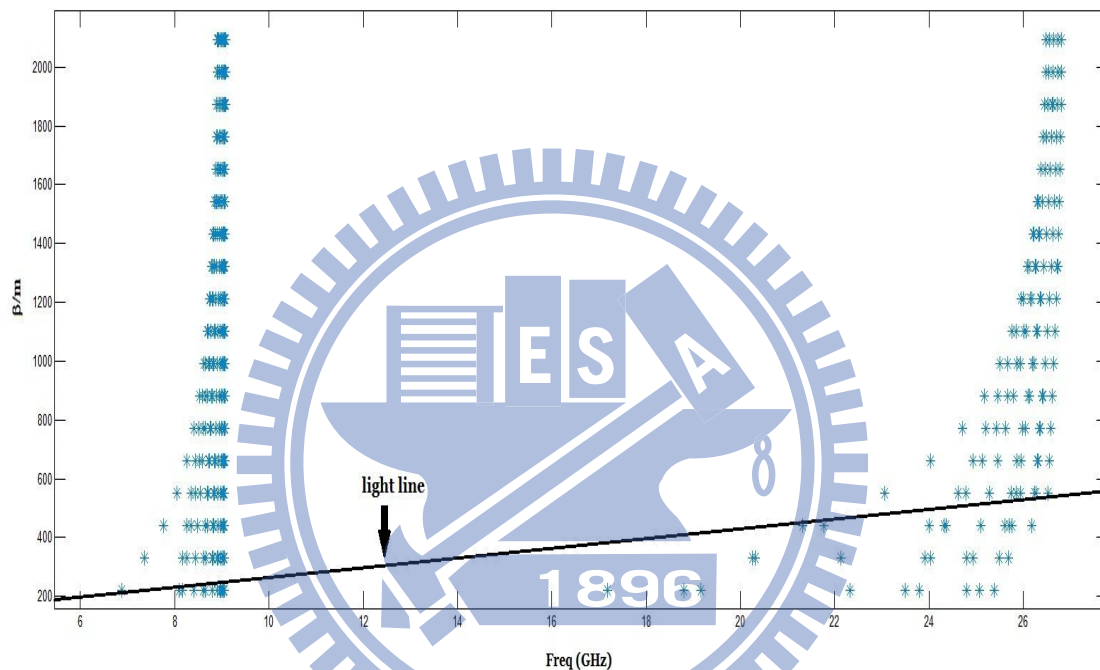

Fig.13   The CST simulation of the Styrofoam material substrate embedded with sidewall pins

Fig. 13 shows the CST simulation result from above fabrication dimension in eigenmode solver. We can notice that it has obvious stop band from about 9.5 ~ 17 GHz. The reason why we are seeking for the dimension which stop band is easily to observed is because we are trying to apply this structure into waveguide filter in the future.

3-2-4 The comparison of the measurement and simulation results of the Styrofoam substrate

Now, we can verify that the characteristic equations have convincible accuracy by these simulation results. After first experiment, we then try to find another dimension which has obvious stopband for that we cannot find any in this dimension setting.

We finally choose the Styrofoam as our sidewall dielectric material with its permittivity 1.27, which is close to free space. Also, we changed the height from 5 mm to 10 mm and it would be easier to measure. The width remained the same, 20 mm.

Next, we fabricate the waveguide with Styrofoam dielectric sidewall and embedded with metallic pins as we designed.

Fig. 14 Perspective view of rectangular waveguide with sidewall dielectric embedded within metallic pins

Since we decide the final dimension of the waveguide, we simulated the dispersion diagram by three different simulation tools to verify their accuracy and find an obvious

stop-band in this structure. However, the experiment still needs the measurement to ensure its credibility. Because of the adaptor WR-90 has its frequency range which would cause distortion beyond or lower the frequency range, 8.2 ~12.4 GHz. Fig. 15 below shows the comparison of the S21 (Insertion loss) between the simulation and the measurement. The blue circle represents the measurement, and the green star shows the simulation by HFSS. Like above described, the measurement processing is limited by the adaptor, and it's accurate from 8.2 to 12.4 GHz. Still, the simulation doesn't have that problem; we still can observe their trends to discuss about where the stop-band of the waveguide would exist.

From about 8.5 GHz to 12 GHz, the trend is telling that the wave can pass through it. They have stop-bands before 8GHz and over 12 GHz. Compare to Fig. 13, we can know that about 8 to 9 GHz, the wave is excited, and after 12 GHz, the insertion loss shows that there would have stop-band. Because we cannot exactly measure the frequency range after 20 GHz, we can still observe the curve trend to assume that would excited again about 17 to 26 GHz like Fig.9 shows.
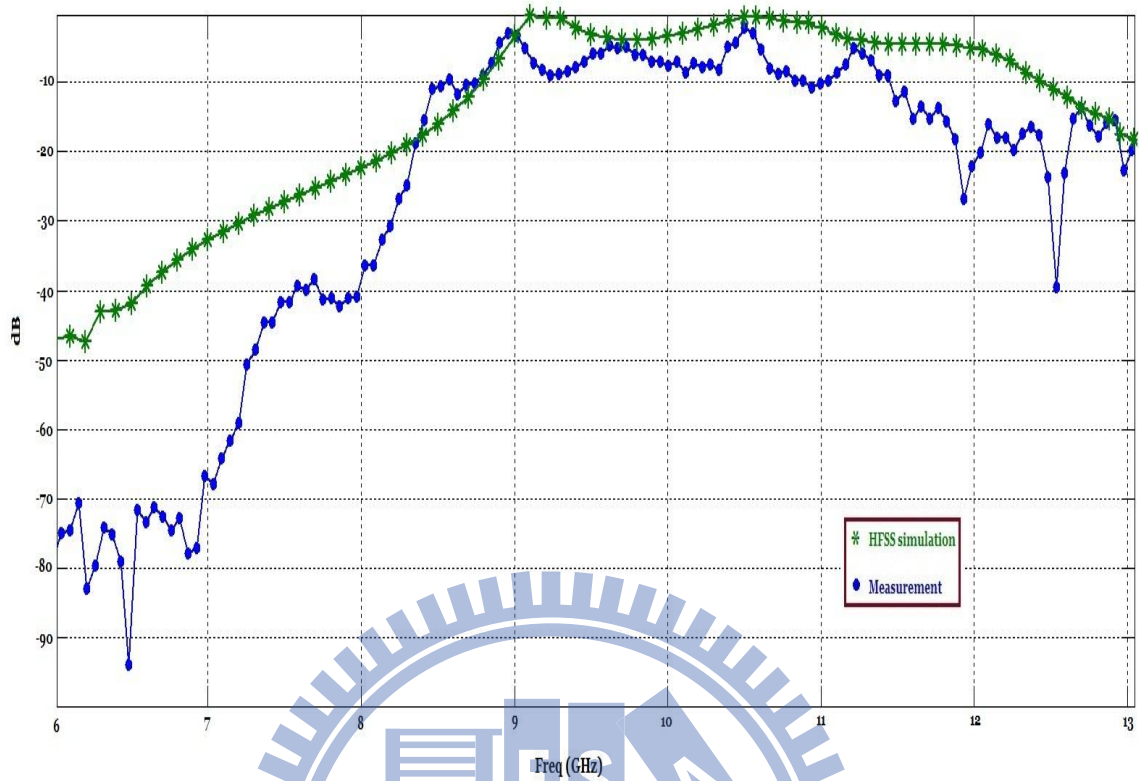
Fig. 15 Comparison of measurement and HFSS simulation in Styrofoam dielectric
sidewall-loaded waveguide

Most of the time, in order to obtain knowledge of just the width and location in the

frequency spectrum of bandgaps of periodic structure, the use of two-port scattering

parameters is more direct than the dispersion diagram.[10]

IV. Conclusion

Recently, there has a new type of novel meta-surfaces, which is called "pin-lattice" or "bed-of-nails". Its characteristics are similar to those of EBG (electromagnetic band-gap) structures, which are well-known for suppressing surface wave propagation in a specific band. Also, the insertion of additional structures into ordinary empty waveguides to tailor the propagation characteristics has been an age-old practice, ranging from the simplest use of dielectric fillings for reduction of cutoff frequency to the plugging in of dielectric layers to serve as impedance match-tunners.

Motivated by the broadband nature of such high-impedance surfaces, it could also be interesting and worthwhile to investigate how such a pin-lattice, when implanted within the sidewall dielectric slab-loading of rectangular waveguide, could affect the bandgap properties.

In this paper, we introduce two similar structures by using vector-potential method and obtain the characteristic equations. Not only verify the accuracy and credibility of the method, but also we find a dimension of the sidewall-loaded embedded with pin-lattice waveguide whose stop band is observable. The above derivation about four cases of vector potential method shows us not only the characteristic equations but also the distribution of electric and magnetic fields. This is an important reason we choose this way to get the characteristic equations instead of TRT.

In the future, we hope we can use it as a waveguide-filter that filters in some frequency range. There has introduction between scattering parameters and dispersion diagram in the reference [10].

Reference

[1]   Per-Simon Kildal, Fellow, IEEE, E. Alfonso, Student Member, IEEE, A. Valero-Nogueira, Member, IEEE, and Eva Rajo-Iglesias, Senior Member, IEEE, *"Local Metamaterial-Based Waveguides in Gaps Between Parallel Metal Plates,"* IEEE ANTENNAS AND WIRELESS PROPAGATION LETTERS, VOL. 8, 2009

[2]   Yi Jia Chiou and Malcolm Ng Mou Kehn, "*Modal Analysis of a Periodic Array of Metallic Pins Embedded within a Grounded Dielectric Substrate – An Asymptotic Solution for Vanishing Unit-Cell Size,*" Institute of Communication Engineering, National Chiao Tung University, Hsinchu, Taiwan

[3]   N. Engheta, R. W. Ziolkowski, Metamaterials Physics and Engineering Explorations, Wiley, New York, 2006.

[4]   D. Sievenpiper, L. Zhang, R. F. J. Broas, N. G. Alexopolous, E.Yablonovitch, "*High-impedance electromagnetic surfaces with a forbidden frequency band,*" IEEE Trans. Microwave Theory

[5]   Carlton H. Walter, "*Traveling wave antennas*", pp.172-183, McGraw-Hill, 1965.

[6]   J. Hirokawa and M. Ando, "Single-layer feed waveguide consisting of posts for plane TEM wave excitation in parallel plates," *IEEE Trans. Antennas Propag.*, vol. 46, no. 5, pp. 625–630, May 1998.

[7]   Alessia Polemi, *Member, IEEE*, Stefano Maci, *Fellow, IEEE*, and Per-Simon Kildal, *Fellow, IEEE, "Dispersion Characteristics of a Metamaterial-Based Parallel-Plate Ridge Gap Waveguide Realized by Bed of Nails,"* IEEE TRANSACTIONS ON ANTENNAS AND PROPAGATION, VOL. 59, NO. 3, MARCH 2011

[8]   Constantine A. Balanis, "*Advanced Engineering Electromagnetics,*" John Wiley &Sons, 2012.

[9]   Malcolm Ng Mou Kehn1*, Eva Rajo-Iglesias2, and Oscar Quevedo-Teruel2," *Waveguide Filters with Multiple Passbands and Stopbands Achieved by Bed of Nails Implanted within Sidewall Dielectric Loadings,"* Department of Electrical Engineering, National Chiao Tung University, Taiwan, Department of Signal Theory & Communication, Carlos III University of Madrid, Spain malcolm.ng@ieee.org, eva@tsc.uc3m.es, oquevedo@tsc.uc3m.es

[10] Yen-ta Lung, "Surface wave dispersion analysis of planar corrugated surfaces by asymptotic corrugations boundary conditions," pp.41-47, Institute of Communications Engineering, National Chiao Tung University